

Transparent nuclei and deuteron-gold collisions at relativistic energies

B. Z. Kopeliovich

Max-Planck Institut für Kernphysik, Postfach 103980, 69029 Heidelberg, Germany,

Institut für Theoretische Physik der Universität, 93040 Regensburg, Germany

and Joint Institute for Nuclear Research, Dubna, 141980 Moscow Region, Russia

(Received 23 July 2003; published 31 October 2003)

The current normalization of the cross section of inclusive high- p_T particle production in deuteron-gold collisions measured at RHIC relies on Glauber model calculations for the inelastic d -Au cross section. These calculations should be corrected for diffraction. Moreover, they miss Gribov's inelastic shadowing which makes nuclei more transparent (color transparency) and reduces the inelastic cross section. The magnitude of this effect rises with energy and one may anticipate it to affect dramatically the normalization of the RHIC data. We evaluate the inelastic shadowing corrections employing the light-cone dipole formalism which effectively sums up multiple interactions in all orders. We found a rather modest correction factor for the current normalization of data for high- p_T hadron production in d -Au collisions. The results of experiments insensitive to diffraction (PHENIX, PHOBOS) should be renormalized by about 20% down, while those which include diffraction (STAR), by only 10%. In spite of smallness of the correction it eliminates the Cronin enhancement in the PHENIX data for pions. The largest theoretical uncertainty comes from the part of inelastic shadowing which is related to diffractive gluon radiation or gluon shadowing. Our estimate is adjusted to data for the triple-Pomeron coupling and is small, however, other models do not have such a restriction and predict much stronger gluon shadowing. Thus, one arrives at quite diverse predictions for the correction factor which may be even as small as $K=0.65$. Therefore, one should admit that the current data for high- p_T hadron production in d -Au collisions at RHIC cannot exclude in a model independent way a possibility of initial state suppression proposed by Kharzeev-Levin-McLerran. To settle this uncertainty one should directly measure the inelastic d -Au cross sections at RHIC. Also, collisions with a tagged spectator nucleon may serve as a sensitive probe for nuclear transparency and inelastic shadowing. We found an illuminating quantum-mechanical effect: the nucleus acts like a lens focusing spectators into a very narrow cone.

DOI: 10.1103/PhysRevC.68.044906

PACS number(s): 24.85.+p, 13.85.Ni, 25.40.Qa

I. INTRODUCTION

Recent data for high- p_T hadron production in deuteron-gold collisions at $\sqrt{s}=200$ GeV at RHIC [1–3] demonstrate importance of these measurements for proper interpretation of data from heavy ion collisions. The observed nuclear effects at high p_T are pretty weak, the enhancement (Cronin effect) measured for pions by PHENIX is only about 10–20%, in accordance with expectation of Ref. [4] and with somewhat larger effect found in Ref. [5], while a suppression, rather than an enhancement was predicted in Ref. [6]. To discriminate between these predictions the data should have at least few percent accuracy.

In this paper we draw attention to the fact that only the shape of p_T distribution was measured experimentally, while the normalization of the data is based on theoretical calculations which are not correct. Therefore, the reported results of deuteron-gold measurements [1–3] may be altered by more appropriate calculations.

The nucleus to nucleon ratio demonstrating the well known Cronin effect [7] is defined as

$$R_{A/N}(p_T) = \frac{d\sigma^{hA}/d^2p_T}{A d\sigma^{hN}/d^2p_T}. \quad (1)$$

At large p_T , of the order of few GeV this ratio exceeds one, but eventually approaches one at very high p_T as is expected according to k_T factorization (it may even drop below one due to the European Muon Collaboration

(EMC) effect at large Bjorken x).

Absolute values of the high- p_T nuclear cross sections are difficult to measure at RHIC, only the fraction of the total inelastic cross section dN^{hA}/d^2p_T is known. Then, one has to normalize it by multiplying the fraction with the total inelastic cross section,

$$R_{A/N}(p_T) = \frac{\sigma_{in}^{hA} dN^{hA}/d^2p_T}{A \sigma_{in}^{hN} dN^{hN}/d^2p_T} = \frac{1}{N_{coll}} \frac{dN^{hA}/d^2p_T}{dN^{hN}/d^2p_T}, \quad (2)$$

where

$$N_{coll} = A \frac{\sigma_{in}^{hN}}{\sigma_{in}^{hA}}. \quad (3)$$

In some experiments the denominator in Eq. (1), $d\sigma^{hN}/d^2p_T$, was directly measured or borrowed from other measurements, otherwise it should be corrected for diffractive dissociation of the colliding protons which possesses a large rapidity gap and escapes detection. In what follows we assume that the denominator in Eq. (1), $d\sigma^{hN}/d^2p_T$, was directly measured (see, however, discussion in Sec. I B 2 and concentrated on nuclear effects, i.e., the inelastic nuclear cross section σ_{in}^{NA} which was calculated in Refs. [1–3] in an oversimplified approach.

A. Number of collisions: What is actually colliding?

The Glauber approach is a model for the elastic hadron-nucleus amplitude. It is demonstrated in Appendix A how to calculate inelastic and quasielastic cross sections using uni-

tarity and completeness. The model does not say anything about exclusive channels of inelastic interaction. One can formally expand the Glauber exponential, and it looks like a series corresponding to different numbers of inelastic collisions of the same hadron and with the same inelastic cross section. However, a high-energy hadron cannot interact inelastically many times, since the very first inelastic collision breaks down coherence between the constituents of the hadron. It takes a long time proportional to the energy to produce a leading hadron in final state.

The cross section of inelastic hadron-nucleus collision, σ_{in}^{hA} , is related to the probability for the incoming hadron to get the very first inelastic collision, usually on the nuclear surface. This is why $\sigma_{in}^{hA} \propto A^{2/3}$. Since the process is fully inclusive, subsequent final state interactions do not affect the cross section due to completeness.

N_{coll} defined via expansion of the Glauber exponential term should not be treated as multiple sequential interactions of the projectile hadron (such as expansion of the exponential describing the time dependence of particle decay does not mean that the particle can decay many times). After the first inelastic interaction the debris of the projectile hadron keep traveling through the nucleus, but their interactions apparently have little to do with the properties of the incoming hadron and its inelastic cross section. Formally, one can relate N_{coll} to the mean number of the Pomerons which undergo unitarity cuts. The Abramovsky-Gribov-Kancheli (AGK) cutting rules [8], which are not proven in QCD, assume that these cuts have the same eikonal weights as given by the Glauber model. In this approach multiple interactions are not sequential (planar), but occur in parallel, i.e., they allow a simultaneous unitarity cut. In terms of the light-cone approach multiple interactions correspond to higher Fock states in the projectile hadron. The constituents of these states propagate through the nucleus and experience their first inelastic interaction independent of each other. The probability of such multiple interactions has little to do with the properties of the low Fock states which dominate the hadron-nucleon cross section, therefore it should not be expressed as a power of σ_m^{hN} . At any rate, whether the AGK weights are correct or not, it is clear that N_{coll} cannot be treated as sequential interactions of the projectile hadron.

The first inelastic collision of the incoming hadron is a soft color-exchange interaction. The projectile partons do not alter either their number (for a given Fock state) or their longitudinal momenta, but the whole system of partons acquires a color. Therefore, the remnants of the hadron turn out to be color connected to the remnants of the target. Then new partons are produced from vacuum (e.g., via the Schwinger mechanism) aiming to neutralize the color of the projectile partons. Their momenta are much smaller than those of the projectile partons. Such an excited and color neutral partonic system keeps propagating through the medium and experiencing new soft color-exchange interactions similar to the ordinary hadrons. The corresponding cross section is subject to color screening and is controlled by the transverse, rather than longitudinal, size of the system.

From the practical point of view, there is nothing wrong in using N_{coll} as a multiplication factor for hard reactions, since

within the Glauber model it is proportional to the nuclear thickness function $T_A^N(b)$, i.e., to the number of opportunities for a parton to perform a hard process. Indeed, the projectile high-energy partons participate in hard reactions independent of the accompanying partons, since color screening plays no role for a hard interaction. Moreover, naively, one may expect that this factor $T_A^N(b)$ (T_{AB} in the case of AB collision) is all one needs to normalize a hard process, and this normalization is independent of the soft cross section σ_{in}^{hN} . However, N_{coll} is defined for events where inelastic collision did happen. Therefore, it must be properly normalized by the probability for the incoming hadron to make inelastic interaction at the given impact parameter:

$$n_{coll}(b) = \frac{\sigma_{in}^{NN} T_A^N(b)}{1 - \exp[-\sigma_{in}^{NN} T_A^N(b)]}. \quad (4)$$

Averaging this expression over inelastic collisions at different impact parameters one indeed arrives to the expression (3).

B. Correcting data for R_{d-Au}

The current analyses of RHIC data [1–3] calculate N_{coll} in the Glauber Monte Carlo model assuming $\sigma_{in}^{NN} = 41–42$ mb. In this paper we challenge these calculations and show that the published results for d -Au collisions are subject to important corrections and the conclusions are model dependent.

There are two major corrections to be done to the Cronin ratio, Eq. (2), measured at RHIC. We combine them in a correction factor K ,

$$R_{dA}(p_T) = R_{dA}^{RHIC}(p_T)K, \quad (5)$$

where

$$K = K_{Gr} K_{Gl}. \quad (6)$$

Here K_{Gr} is the correction related to Gribov's inelastic shadowing missed in Glauber model calculations. It is introduced in the following section and calculated throughout the paper.

Even within the Glauber model the calculations performed in Refs. [1–3] should be corrected by a factor K_{Gl} . It originates from a more accurate treatment of the inelastic NN cross section which should correspond to the class of events selected for the analysis, as is explained in Sec. I B 2. This correction is calculated in Sec. II.

There is an additional correction which should be included into Eq. (6) if one needs to compare with theoretical predictions for the Cronin effect for pA collisions. It is related to the fact that the deuteron is a nucleus and is also subject to the Cronin effect. Therefore high- p_T enhancement in $d-A$ must be somewhat stronger than in $p-A$ collisions. This correction is evaluated in Sec. VII and found rather small.

1. Inelastic shadowing

It is known that Gribov's inelastic corrections [9] to the Glauber approximation make nuclear matter more transparent and reduce the hadron-nucleus cross sections compared to the Glauber model. This effect steeply rises with energy,

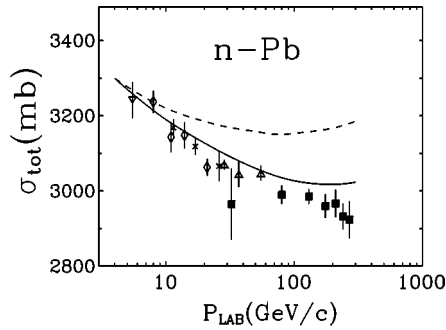


FIG. 1. Data and calculations [10] for the total neutron-lead cross section as a function of energy. The dashed curve corresponds to the Glauber model, while the solid curve is corrected for Gribov's inelastic shadowing.

as one can see from the example depicted in Fig. 1 for the total neutron-lead cross section measured and calculated in Ref. [10]. Apparently, the Glauber model overestimates the cross section, and the deviation rises with energy. Without a good theoretical input one cannot predict what will happen at the energy of RHIC, which is 100 times higher than in fixed-target experiments at Fermilab. This is a serious challenge for the theory to calculate the inelastic dA cross section at these energies, and the results apparently will be model dependent. However, it is certain that the sign of the correction remains negative and it can only rise with energy, i.e., it cannot be smaller than what is shown in Fig. 1 for low energies.

Our own estimates summarized in Table I give a moderate reduction, about 20%. The weakness of the effect is based on a proper treatment of diffraction and is fixed by data on large mass diffractive dissociation of protons [11]. At the same time, many models predict quite a strong gluon shadowing even at high virtualities. Naturally, this effect should not be weaker in soft NN interactions. Then it may lead to a stronger suppression of the inelastic dA cross section than that we found, as is discussed in Sec. VI B.

Note that although inelastic shadowing makes nuclear medium more transparent, the mean number of collisions increases according to Eq. (3). It sounds counterintuitive that a hadron experiences more collisions in a less absorptive medium. Formally it follows from Eq. (3), but can be explained qualitatively. For instance, if one calculated the mean number of collisions in a photoabsorption reaction on a nucleus using the Glauber formula, the result would be very small, proportional to α_{em} . However, N_{coll} is defined for events when inelastic collision takes place. In this case it comes from hadronic fluctuations of the photon and is much larger than the number of collisions given by the Glauber formulas, Eq. (3). This example explains why N_{coll} increases due to inelastic shadowing.

2. How inelastic is the inelastic cross section?

As far as the need to calculate the deuteron-nucleus inelastic cross section is concerned it should be done in correspondence with the class of events selected by the trigger. The cross section calculated via the Glauber Monte Carlo

generator in all three experiments corresponds to the Glauber formula derived in Appendix A, Eq. (A14), where σ_{in}^{NN} is the total inelastic NN cross section. Then, according to derivation, Eq. (A14) describes the total inelastic cross section on a nucleus minus the part related to quasielastic nuclear excitations (with no hadron produced). This is not what was actually measured in any of the three experiments [1–3]. These experiments have different event selections and the calculations should comply with that.

The STAR experiment triggers on forward neutrons from the gold [2] and detects all inelastic d -Au collisions including quasielastic excitation of the gold.¹ In this case, according to the Glauber formalism presented in Appendix A, one should rely on Eq. (A10) with $\sigma_{tot}^{NN}=51$ mb, rather than $\sigma_{in}^{NN}=42$ mb. At the same time, the two other spectrometers, PHENIX and PHOBOS, seem to be insensitive to large rapidity gap events, i.e., diffractive excitations of the deuteron and gold [1,3].² Then Eq. (A14) should be applied with a replacement $\sigma_{in}^{NN} \Rightarrow \sigma_{in}^{NN} - 2\sigma_{sd}^{NN} - \sigma_{dd}^{NN} \approx 30$ mb, i.e., the single and the double diffraction must be subtracted (see details in Sec. II [12,13]). Apparently, it makes difference whether one performs calculations with input cross section 51 mb, 42 mb, or 30 mb.

The numerator in Eq. (4), σ_{in}^{NN} , is even more sensitive than the denominator to assumptions where inelastic channels should be included. However this does not seem to be a problem, since the cross section of high- p_T production in pp collisions, $d\sigma^{pp}/d^2p_T$, was directly measured in all the three experiments,³ and we consider only the nuclear modification factor, Eq. (5), in what follows.

C. The outline

This paper is organized as follows. We present a brief and simple derivation of basic formulas of the Glauber model [16] in Appendix A. In Sec. II we treat the deuteron as a nucleus and generalize the Glauber model for this case. We derive formulas for the cross sections of different channels, perform numerical calculations, and present the results in Table I. We corrected the input inelastic NN cross section for diffraction and found a smaller σ_{in}^{dA} than in Refs. [1,3], but larger than in Ref. [2].

Events with a tagged spectator nucleon may serve as a sensitive probe for nuclear transparency, since the spectator

¹I appreciate the very informative communication with Carl Gagliardi on this issue.

²A part of diffraction might have been included into the trigger efficiency of the PHENIX spectrometer; namely, double diffraction, i.e., excitation of nucleons in both the deuteron and the gold can reach and fire sometimes the closest of the two beam counter (BBC) triggers covering pseudorapidity intervals $\eta = \pm(3-3.9)$. However, the main part of diffraction, single diffractive excitation of either the deuteron, or gold could hardly reach the opposite hemisphere and fire both the BBC triggers simultaneously, which is the trigger condition. I am thankful to Barbara Jacak and Sasha Milov for informative and clarifying discussions on this issue.

³Although it is stated in Ref. [1] that the cross section $d\sigma^{pp}/d^2p_T$ was normalized to 42 mb, it was measured [14,15].

TABLE I. Results for different cross sections and numbers of collisions calculated using Glauber approximation (Sec. II), corrected for inelastic shadowing related to valence quark fluctuations (Sec. V A), and for gluon shadowing (Sec. VI). The results including the ultimate renormalization factor K depend on the experimental setup and are different for the STAR and PHENIX experiments.

	Observable	Glauber model	Valence quark fluctuations	Plus gluonic excitations	Correction factor
STAR	σ_{tot}^{d-Au} (mb)	4110.1	3701.0	3466.2	
	σ_{in}^{d-Au} (mb)	2422.7	2226.6(2335.8)	2118.3(2228.3)	
	Factor K in Eqs. (5) and (6)	$K_{GL}=1.04$		$K_{Gr}=0.87(0.92)$	$K=0.91(0.96)$
	N_{coll}^{in} (minimum bias)	6.9	7.5	7.9	
	σ_{in}^{d-Au} (tagg)(mb)	458.4	544.9(511.5)	551.8(520.1)	
PHENIX	N_{coll}^{in} (tagg)	2.9	4.4	5.0	
	$\sigma_{nondiff}^{d-Au}$ (mb)	2146.0	1998.3(2100.1)	1930.3(2033.7)	
	Factor K	$K_{GI}=0.92$		$K_{Gr}=0.9(0.95)$	$K=0.83(0.87)$
	$N_{coll}^{nondiff}$ (minimum bias)	5.5	5.9	6.1	
	$\sigma_{nondiff}^{d-Au}$ (tagg)(mb)	324.3	480.2(451.5)	498.4(470.6)	
	$N_{coll}^{nondiff}$ (tagg)	2.3	2.9	3.2	

must propagate through the nucleus with no interaction. We calculate the total cross section for this channel and the transverse momentum distribution of the spectators. Contrary to naive expectation that noninteracting nucleons retain their primordial Fermi momentum distribution, we found an amazingly strong focusing effect; namely, the nucleus acts like a lens focusing the spectators into a narrow cone with momentum transfer range of the order of the inverse nuclear radius. The transverse momentum spectrum of the spectators acquires typical diffraction structure having minima and maxima.

Inelastic shadowing corrections are introduced in Sec. IV. First, we use the traditional presentation in terms of inelastic diffractive excitations in intermediate state of hadron-nucleus elastic amplitude (Sec. IV A). This approach is quite restricted, being unable to deal with higher order scattering terms which are especially important at high energies. Therefore, we switch to the eigenstate representation introduced in general terms in Sec. IV B. Its realization in QCD is the light-cone color-dipole approach presented in Sec. V.

The part of the inelastic corrections related to the lowest hadronic Fock component consisting only of valence quarks corresponds to diffractive excitation of resonances in usual terms. This contribution is analyzed and estimated numerically in Sec. V A. We demonstrate that these corrections make heavy nuclei much more transparent: instead of exponential attenuation we found a linear dependence on the inverse nuclear thickness (Sec. V A 1). Correspondingly, we derived formulas for cross sections of different channels corrected for inelastic shadowing for hadron-nucleus (Sec. V A 2), and deuteron-nucleus (Sec. V A) collisions. In Sec. V C we study the possibility of improving our calculations. We tested sensitivity of our results to the form of the nucleon wave function and derived formulae for the case of a realistic saturated dipole-nucleon cross section.

Gluonic excitations corresponding to Fock states containing extra gluons are considered in Sec. VI. They correspond to diffractive excitations of large mass which are known to have quite a small cross section. This smallness leads to a

prediction of rather weak gluonic shadowing, $\sim 20\%$, and small contribution to the inelastic corrections. At the same time other models predict much stronger gluon shadowing (Sec. VI B) which may substantially change the normalization of the d -Au data.

Since nuclear matter becomes more transparent due to inelastic shadowing, the number of participants changes as well. In Sec. VI C we found this effect to be sizable.

In Sec. VII we sum up the effects considered so far to see how much they affect the d -Au data. The results are presented in Table I. We also corrected the PHENIX data for high- p_T pions to see how important these corrections are compared to the current error bars. We found a considerable change: the Cronin effect for high- p_T pions had disappeared.

Our observations are summarized in Sec. VIII. The main conclusion is that the current data for high- p_T hadron production in deuteron-gold collisions are not decisive, and should be complemented with direct measurements of the inelastic d -Au cross section.

II. EXTENDING THE GLAUBER MODEL TO DEUTERON-NUCLEUS COLLISIONS

The basic formulas of the Glauber model for hadron-nucleus collisions are presented in Appendix A. If one treats the deuteron as a hadron, one can calculate the dA total, total elastic, and inelastic cross section, provided that the elastic dN amplitude is known. The latter can be calculated employing the Glauber model, too. This is done in Appendix A.

One can do calculations differently, treating the deuteron as a system of two nucleons interacting with the nucleus. In this case one can consider more reaction channels as deuteron excitation, etc., which have been missed in the previous approach.

A. The total cross section

We generalize Eq. (A5) from Appendix A for a deuteron beam as follows:

$$\begin{aligned}\sigma_{tot}^{dA} &= 2 \operatorname{Re} \int d^2 r_T |\Psi_d(r_T)|^2 \langle 0 | 1 - \prod_{k=1}^A [1 - \Gamma^{pN}(\vec{b} - \vec{r}_T/2 - \vec{s}_k)] [1 - \Gamma^{nN}(\vec{b} + \vec{r}_T/2 - \vec{s}_k)] | 0 \rangle \\ &= 2 \int d^2 b \int d^2 r_T |\Psi_d(r_T)|^2 \left(1 - \exp \left\{ -\frac{1}{2} \sigma_{tot}^{NN} \left[T_A^N \left(\vec{b} + \frac{1}{2} \vec{r}_T \right) + T_A^N \left(\vec{b} - \frac{1}{2} \vec{r}_T \right) \right] + \sigma_{el}^{NN} T_A^N(b) \exp \left(-\frac{r_T^2}{4B_{NN}} \right) \right\} \right),\end{aligned}\quad (7)$$

where \vec{r}_T is the transverse nucleon separation in the deuteron and $|\Psi_d(r_T)|^2$ is the deuteron light-cone wave function squared and integrated over relative sharing by the nucleons of the deuteron longitudinal momentum. It is presented in Appendix B. The effective nuclear thickness function $T_A^N(b)$ convoluted with the NN elastic amplitude is introduced in Eq. (A6).

We did calculations with nuclear density in the Woods-Saxon form

$$\rho_A(r) = \frac{3A}{4\pi R_A^3 (1 + \pi^2 a^2/R_A^2)} \frac{1}{1 + \exp\left(\frac{r - R_A}{a}\right)}, \quad (8)$$

with $R_A = 6.38$ fm and $a = 0.54$ fm, same as in Ref. [1] for easier comparison. The result for the total cross section σ_{tot}^{d-Au} is shown in Table I.

Equation (7) is easy to interpret. The first two terms in the exponent correspond to independent interaction of two nucleons separated by transverse distance \vec{r}_T . Of course, the

smaller r_T is, the stronger nucleons shadow each other, and this is accounted for by the third term.

One can see the difference between this expression and Eq. (A5) (for $h \equiv d$). In the latter case the averaging over \vec{r}_T is put up into the exponent, while in the former case, Eq. (7), the whole exponential is averaged. We will see in Sec. IV B that this difference is a part of Gribov's inelastic corrections, so Eq. (7) takes the first step beyond the Glauber approximation.

Note that the last term in the exponent in Eq. (7) is quite small. Besides smallness of $\sigma_{el}^{NN}/\sigma_{tot}^{NN}$, the exponential factor is rather small. The mean value of the exponent is $\langle r_T^2 \rangle / 4B_{NN} \approx 5$. This term reduces the total d -Au cross section by 1.3% only.

B. The cross section of elastic dA scattering and deuteron breakup $dA \rightarrow pnA$

According to Eq. (A9) in order to find elastic dA cross section one should square the partial elastic amplitude and integrate over b :

$$\sigma_{el}^{dA} = \int d^2 b \left| \int d^2 r_T |\Psi_d(r_T)|^2 \left(1 - \exp \left\{ -\frac{1}{2} \sigma_{tot}^{NN} \left[T_A^N \left(\vec{b} + \frac{1}{2} \vec{r}_T \right) + T_A^N \left(\vec{b} - \frac{1}{2} \vec{r}_T \right) \right] + \sigma_{el}^{NN} T_A^N(b) \exp \left(-\frac{r_T^2}{4B_{NN}} \right) \right\} \right) \right|^2. \quad (9)$$

This is the square of the average of the elastic amplitude over deuteron configurations. If, however, we take average of the amplitude squared, the result will include also dissociation $d \rightarrow pn$, i.e.,

$$\begin{aligned}\sigma_{el}^{dA}(dA \rightarrow dA) + \sigma_{diss}^{dA}(dA \rightarrow npA) &= \int d^2 b \int d^2 r_T |\Psi_d(r_T)|^2 \\ &\times \left| 1 - \exp \left\{ -\frac{1}{2} \sigma_{tot}^{NN} \left[T_A^N \left(\vec{b} + \frac{1}{2} \vec{r}_T \right) + T_A^N \left(\vec{b} - \frac{1}{2} \vec{r}_T \right) \right] + \sigma_{el}^{NN} T_A^N(b) \exp \left(-\frac{r_T^2}{4B_{NN}} \right) \right\} \right|^2.\end{aligned}\quad (10)$$

C. The total inelastic cross section

Subtracting from the total cross section the elastic part one gets the cross section of all inelastic channels in dA . We, however, prefer to subtract the deuteron quasielastic breakup too, since it is not detected by any of the RHIC experiments. Then we have

$$\begin{aligned}\sigma_{in}^{dA} &= \sigma_{tot}^{dA} - \sigma_{el}^{dA} - \sigma_{diss}^{dA}(dA \rightarrow npA) \\ &= \int d^2 b \int d^2 r_T |\Psi_d(r_T)|^2 \times \left(1 - \exp \left\{ -\frac{1}{2} \sigma_{tot}^{NN} \left[T_A^N \left(\vec{b} + \frac{1}{2} \vec{r}_T \right) + T_A^N \left(\vec{b} - \frac{1}{2} \vec{r}_T \right) \right] + 2\sigma_{el}^{NN} T_A^N(b) \exp \left(-\frac{r_T^2}{4B_{NN}} \right) \right\} \right).\end{aligned}\quad (11)$$

The result of numerical calculation for this cross section is exposed in Table I. This cross section covers diffractive excitations as well, therefore we place the result in the upper part of the table which is supposed to be related to experiments sensitive to diffraction (STAR).

The impact parameter distribution of the inelastic cross section is plotted by a dashed curve in Fig. 2 and the integrated cross section is shown in Table I.

D. The cross section of nondiffractive channels

In experiments insensitive to large rapidity gap event one should employ the inelastic cross section with all diffractive contributions removed; that is one should also subtract the cross sections of quasielastic excitation of the nucleus, $A \rightarrow A^*$, and diffractive excitation of colliding nucleons.

The cross section of single ($dA \rightarrow dA^*$) and double ($dA \rightarrow pdA^*$) quasielastic and quasidiffractive nuclear excitation reads [compare with Eq. (A13)]

$$\begin{aligned}
 & \sigma_{qel}^{dA}(dA \rightarrow dA^*) + \sigma_{qsd}^{dA}(dA \rightarrow pnA^*) \\
 &= \int d^2 r_T |\Psi_d(r_T)|^2 \times \left\{ \langle 0 | \left| 1 - \prod_{k=1}^A [1 - \Gamma^{pN}(\vec{b} - \vec{r}_T/2 - \vec{s}_k)][1 - \Gamma^{nN}(\vec{b} + \vec{r}_T/2 - \vec{s}_k)] \right|^2 | 0 \rangle \right. \\
 & \quad \left. - \langle 0 | 1 - \prod_{k=1}^A [1 - \Gamma^{pN}(\vec{b} - \vec{r}_T/2 - \vec{s}_k)][1 - \Gamma^{nN}(\vec{b} + \vec{r}_T/2 - \vec{s}_k)] | 0 \rangle^2 \right\} \\
 &= \int d^2 b \int d^2 r_T |\Psi_d(r_T)|^2 \left(\exp \left\{ -\sigma_{in}^{NN} \left[T_A^N \left(\vec{b} + \frac{1}{2} \vec{r}_T \right) + T_A^N \left(\vec{b} - \frac{1}{2} \vec{r}_T \right) \right] + 4\sigma_{el}^{NN} T^N(b) \gamma(r_T) \exp \left(-\frac{r_T^2}{4B_{NN}} \right) \right\} \right. \\
 & \quad \left. - \exp \left\{ -\sigma_{tot}^{NN} \left[T_A^N \left(\vec{b} + \frac{1}{2} \vec{r}_T \right) + T_A^N \left(\vec{b} - \frac{1}{2} \vec{r}_T \right) \right] + \sigma_{el}^{NN} T^N(b) \exp \left(-\frac{r_T^2}{4B_{NN}} \right) \right\} \right), \tag{12}
 \end{aligned}$$

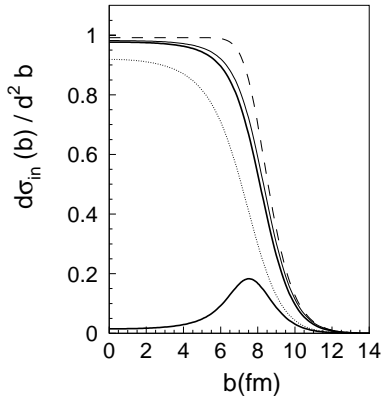


FIG. 2. The impact parameter distribution of inelastic deuteron-gold collisions (three upper curves) including diffractive excitations (STAR trigger). Impact parameter \vec{b} corresponds to the center of gravity of the deuteron. The dashed curve corresponds to the Glauber approximation, Eq. (10). The thin solid curve includes inelastic shadowing related to excitation of the valence quark skeleton, Eq. (45). The thick solid curve is final, it includes gluon shadowing as well. The bottom solid thick curve shows the difference between the Glauber and final curves. The dotted curve shows the range of model uncertainty and corresponds to gluon shadowing with $R_G=03$ (see Sec. VI B). All curves are calculated with total cross section $\bar{\sigma}_{tot}^{NN}=51$ mb.

where

$$\gamma(r) = 1 - \frac{8}{3} \frac{\sigma_{el}^{NN}}{\sigma_{tot}^{NN}} \exp \left(-\frac{r_T^2}{8B_{NN}} \right) + 8 \left(\frac{\sigma_{el}^{NN}}{\sigma_{tot}^{NN}} \right)^2 \exp \left(-\frac{r_T^2}{4B_{NN}} \right) \tag{13}$$

is a correction factor hardly different from 1. In what follows we do not keep the small terms in Eq. (13). Note that the form of Eq. (12) is analogous to that of Eq. (A13).

For experiments insensitive to diffraction the quasielastic cross section, Eq. (12), should be subtracted from Eq. (11) and the result would be similar to Eq. (A14). However, we still miss the contribution of diffractive channels related to diffractive excitations of nucleons in the deuteron and nucleus. It is impossible to introduce consistently diffraction in the framework of the Glauber model which is a single-channel approximation. Diffraction naturally emerges in the multiple coupled channel approach or in the eigenstate method introduced below. Meanwhile, one can use the following prescription.

Let us expand the exponentials in Eq. (12) in small expansion parameter $\sigma_{el}^{NN} T_A(b)$ up to the first order,

$$\begin{aligned} \sigma_{qel}^{dA} \approx & \int d^2b \int d^2r_T |\Psi_d(r_T)|^2 \exp \left\{ -\sigma_{tot}^{NN} \left[T_A^N \left(\vec{b} + \frac{1}{2} \vec{r}_T \right) \right. \right. \\ & \left. \left. + T_A^N \left(\vec{b} - \frac{1}{2} \vec{r}_T \right) \right] \right\} \sigma_{el}^{NN} \left[T_A^N \left(\vec{b} + \frac{1}{2} \vec{r}_T \right) \right. \\ & \left. + T_A^N \left(\vec{b} - \frac{1}{2} \vec{r}_T \right) \right] + \dots \end{aligned} \quad (14)$$

In order to include the possibility of diffractive excitation of nucleons in the colliding nuclei, one should replace in Eq. (14),

$$\sigma_{el}^{NN} \Rightarrow \tilde{\sigma}_{el}^{NN} = \sigma_{el}^{NN} + 2\sigma_{sd}^{NN} + \sigma_{dd}^{NN} \quad (15)$$

in all orders of $\sigma_{el}^{NN} T_A(b)$. This is a substantial correction since at RHIC energy $\sigma_{el}^{NN} = 9$ mb, and $\sigma_{el}^{NN} + 2\sigma_{sd}^{NN} + \sigma_{dd}^{NN} = 21$ mb.

The final Glauber model expression for the nondiffractive inelastic dA cross section reads

$$\begin{aligned} \sigma_{nondiff}^{dA} = & \int d^2b \int d^2r_T |\Psi_d(r_T)|^2 \\ & \times \left(1 - \exp \left\{ -\tilde{\sigma}_{in}^{NN} \left[T_A^N \left(\vec{b} + \frac{1}{2} \vec{r}_T \right) \right. \right. \right. \\ & \left. \left. + T_A^N \left(\vec{b} - \frac{1}{2} \vec{r}_T \right) \right] \right\} + 4\tilde{\sigma}_{el}^{NN} T_A^{NN}(b) \exp \left(-\frac{r_T^2}{4B_{NN}} \right) \right), \end{aligned} \quad (16)$$

where

$$\tilde{\sigma}_{in}^{NN} = \sigma_{tot}^{NN} - \tilde{\sigma}_{el}^{NN}. \quad (17)$$

We calculated the nondiffractive part, Eq. (16), of the inelastic d -Au cross section and the result is shown in Table I. The corresponding number of collisions also presented in the table is rather small compared to the one quoted in Ref. [1]. This is mainly due to a smaller inelastic cross section $\tilde{\sigma}_{in}^{NN}$ we use.

III. QUANTUM MECHANICS AT WORK: ILLUMINATING FOCUSING EFFECT FOR SPECTATORS

Assume that only the proton in the deuteron interacts inelastically with the nucleus, while the neutron is a spectator (of course, all the following results are symmetric relative to interchange $p \leftrightarrow n$). This is a very interesting process of simultaneous interaction and no interaction. It provides direct information about nuclear transparency. Apparently, this process pushes the neutron to the ultraperiphery of the nucleus where its survival probability is high, while the proton prefers to hit the dense area of the nucleus and interact.

Naively, the survived spectator neutrons should maintain their primordial transverse momentum distribution controlled by the deuteron size. This is assumed in the Glauber Monte Carlo. However, quantum mechanics is at work, and the nucleus acts like a lens focusing spectator neutrons. The survival probability modifies the shape of the wave packet of the spectators in the impact parameter plane. Correspond-

ingly, their p_T distribution changes. This is how elastic scattering on an absorptive target happens: it is not due to transparency of the target, but is caused by absorption. In the limit of a completely transparent target, the incoming plane wave is not disturbed and no scattering occurs. Absorption makes a hole in the plane wave, and one can think about the outside area of the incoming wave which undergoes elastic scattering. On the other hand, one can subtract the incoming plane wave whose Fourier transform is just a δ function (zero angle scattering) and the rest is a wave packet with a transverse area of the target size. A Fourier transform of this wave packet gives the elastic amplitude [compare with Eq. (A9)].

Thus, the spectator neutrons experience elastic scattering on the target, rather than simply propagating with the undisturbed primordial transverse Fermi momentum. Below, we derive formulas which show how elastic scattering of the spectator neutrons happens and perform numerical evaluation of the effect.

We start with the cross section of this process which can be written as

$$\begin{aligned} \sigma_{tagg}^{dA}(dA \rightarrow nX) = & \text{Re} \int d^2r_T |\Psi_d(r_T)|^2 \\ & \times \langle 0 | \prod_{k=1}^A [1 - \Gamma^{NN}(\vec{b} - \vec{r}_T - \vec{s}_k)]^2 \\ & \times \left\{ 1 - \prod_{k=1}^A [1 - 2\Gamma^{pN}(\vec{b} - \vec{s}_k)] \right\} |0\rangle, \end{aligned} \quad (18)$$

where \vec{b} is the impact parameter of the proton. The first factor here would be the elastic neutron-nucleus cross section, if it were not weighted by the second term which is the inelastic proton-nucleus cross section, i.e., the difference between the total and elastic and quasielastic cross sections (see Appendix A).

After integration over the coordinates of bound nucleons we get

$$\begin{aligned} \sigma_{nondiff}^{tagg}(dA \rightarrow nX) = & \int d^2b \int d^2r_T |\Psi_d(r_T)|^2 \\ & \times \exp \left[-\sigma_{tot}^{NN} T_A^N \vec{b} - \vec{r}_T \right] \\ & \times \left\{ 1 - \exp \left[-\tilde{\sigma}_{in}^{NN} T_A^N(b) + 4\sigma_{el}^{NN} T^N \right. \right. \\ & \left. \left. \times (\vec{b} - \vec{r}_T/2) \chi(r_T) \exp \left(-\frac{r_T^2}{4B_{NN}} \right) \right] \right\}. \end{aligned} \quad (19)$$

Here we made a correction for diffractive channels replacing $\sigma_{in}^{NN} \Rightarrow \tilde{\sigma}_{in}^{NN}$ and $\sigma_{el}^{NN} \Rightarrow \tilde{\sigma}_{el}^{NN}$, valid only for those experiments which are not sensitive to diffraction (PHENIX, PHOBOS). Correspondingly, the numerical result for $\sigma_{nondiff}^{tagg}(dA \rightarrow nX)$ is placed at the bottom part of the table. The results at the upper part of the table use the total elastic and total cross sections instead of $\tilde{\sigma}_{el}^{NN}$ and $\tilde{\sigma}_{in}^{NN}$ as

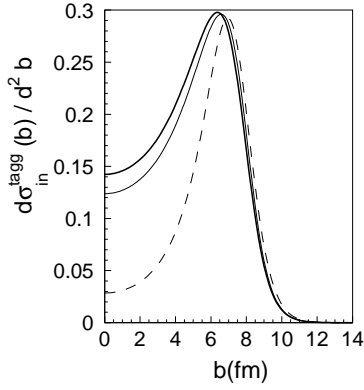


FIG. 3. The impact parameter distribution of interacting protons in tagged deuteron-gold collisions with spectator neutrons. The calculation includes diffractive excitations (STAR trigger). Impact parameter \vec{b} corresponds to the proton. The dashed curve represents the Glauber approximation, Eq. (10). The thin solid curve includes inelastic shadowing related to excitation of the valence quark skeleton, Eq. (45). The thick solid curve includes gluon shadowing as well. All curves are calculated with total cross section $\bar{\sigma}_{tot}^{NN} = 51$ mb.

an input for calculations. Indeed, since the STAR experiment is sensitive to quasielastic nuclear excitation as well, it should be included, and one has to rely on Eq. (A13). We also demonstrate the impact parameter dependence of $\sigma_{in}^{tagg}(dA \rightarrow nX)$ in Fig. 3. Interestingly, the interacting protons in tagged dA collisions strongly pick at the very edge of the nucleus in spite of the large radius of the deuteron. This is not a trivial observation and can be probably interpreted as follows. The spectator neutron must be mostly outside of the nucleus. Then, for protons which are close to the edge of the nucleus the interval of azimuthal angle between the proton and the neutron is larger than for a proton deep inside the nuclear area. This phase space factor enhances the contribution of peripheral protons.

To see how the spectator neutrons are distributed one can use the same equation (19) with the replacement $\vec{b} \Rightarrow \vec{b} + \vec{r}_T$. The result of calculations is depicted in Fig. 4. This plot demonstrates that the spectators have a more peripheral impact parameter distribution than the interacting protons, but they are amazingly close.

We also calculated the number of collisions of the proton which underwent interaction in events with a tagged spectator neutron,

$$N_{coll}^{tagg} = \frac{\bar{\sigma}_{in}^{NN}}{\sigma_{tagg}^{dA}} \int d^2b \int d^2r_T |\Psi_d(r_T)|^2 T_A^N(\vec{b} + \vec{r}_T/2) \times \exp[-\sigma_{tot}^{NN} T_A^N(\vec{b} - \vec{r}_T/2)]. \quad (20)$$

The results for N_{coll}^{tagg} for events which include diffraction or not are shown at the upper and bottom parts of Table I respectively. The mean value of N_{coll} for tagged events turns out to be nearly a half of the minimal bias value, Eq. (3), which is for two nucleons in the deuteron. This contradicts the intuitive expectation that tagged events are

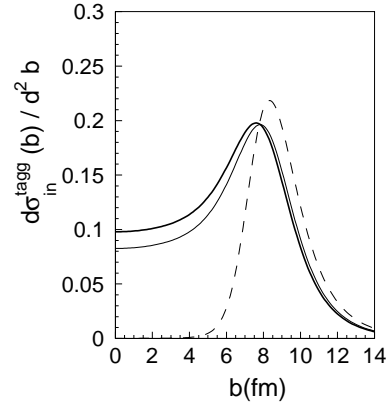


FIG. 4. The impact parameter distribution of spectator neutrons in tagged deuteron-gold collisions with interacting protons. The calculation includes diffractive excitations (STAR trigger). Impact parameter \vec{b} corresponds to the proton. The dashed curve represents the Glauber approximation, Eq. (10). The thin solid curve includes inelastic shadowing related to excitation of the valence quark skeleton, Eq. (45). The thick solid curve includes gluon shadowing as well. All curves are calculated with total cross section $\bar{\sigma}_{tot}^{NN} = 51$ mb.

much more peripheral than minimum bias inelastic collisions and the proton should have a much smaller number of collisions.

To get the transverse momentum distribution of spectator neutrons, one should Fourier transform the elastic neutron amplitude before squaring it:

$$\begin{aligned} \frac{d\sigma_{tagg}(dA \rightarrow nX)}{d^2q_T} &= \frac{1}{(2\pi)^2} \int d^2b \{1 - \exp[-\bar{\sigma}_{in}^{NN} T_A^N(b)]\} \\ &\times \int d^2r_1 d^2r_2 \times \exp[i\vec{q}_T(\vec{r}_1 - \vec{r}_2)] \\ &\times \exp\left\{-\frac{1}{2}\bar{\sigma}_{tot}^{NN}[T_A^N(\vec{b} - \vec{r}_1) + T_A^N(\vec{b} - \vec{r}_2)]\right\} \\ &\times \int_{-\infty}^{\infty} dr_L \left[\frac{u^*(r_L, r_1)u(r_L, r_2) + w^*(r_L, r_1)w(r_L, r_2)}{\sqrt{(r_L^2 + r_1^2)(r_L^2 + r_2^2)}} \right]. \end{aligned} \quad (21)$$

It is important that the proton inelastic interaction is incoherent, therefore we should first sum up coherently all amplitudes of neutron elastic scattering for the fixed impact parameter of the proton, then Fourier transform it, square and after all integrate over the proton impact parameter. This is explicitly done in Eq. (21). Apparently, integration over \vec{q}_T in Eq. (21) leads to the expression in Eq. (19). The S and D wave functions are presented in Appendix B.

In Fig. 5 we compare the normalized differential cross section, Eq. (21),

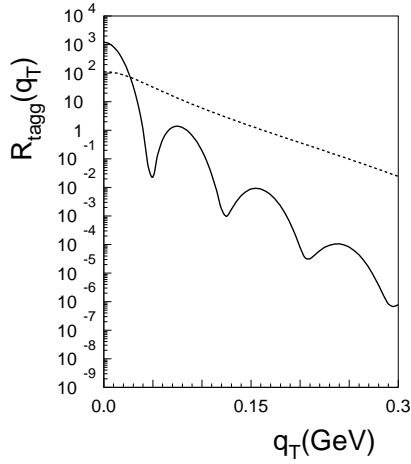


FIG. 5. Transverse momentum distribution of spectator neutrons in the tagged reaction $d+Au \rightarrow n+X$ (solid curve), and in the projectile deuteron (dashed curve). The inelastic reaction $p+Au \rightarrow X$ is assumed to include diffraction (STAR experiment). The calculations are performed in the Glauber approximation, Eq. (21).

$$R_{tagg}(q_T) = \frac{1}{\sigma_{in}^{tagg}} \frac{d\sigma_{tagg}^{dA}}{d^2q_T}, \quad (22)$$

with the undisturbed primordial distribution of the neutron in the incoming deuteron, also normalized to 1,

$$\begin{aligned} \frac{dN_n^d}{d^2q} &= \frac{1}{(2\pi)^2} \int d^2r_1 d^2r_2 \exp[i\vec{q}_T(\vec{r}_1 - \vec{r}_2)] \\ &\times \int_{-\infty}^{\infty} dr_L \left[\frac{u^*(r_L, r_1)u(r_L, r_2) + w^*(r_L, r_1)w(r_L, r_2)}{\sqrt{(r_L^2 + r_1^2)(r_L^2 + r_2^2)}} \right], \end{aligned} \quad (23)$$

The surprising observation is that the spectator neutrons have a much narrower q_T distribution than the Fermi motion in the deuteron. This is opposite to the usual q_T broadening (Cronin effect) for particles propagating through a matter [17]. In the present case the nucleus acts like a lens focusing neutrons. Figure 5 also exposes quite a different shape of the q_T distribution of spectators having diffractionlike minima and maxima.

Comparing the mean values of q_T^2 of spectator neutrons with the primordial value in the deuteron, the difference is tremendous, about factor of 20,

$$\langle q_T^2 \rangle_{spect} = 0.00038 \text{ GeV}^2, \quad (24)$$

$$\langle q_T^2 \rangle_{deuteron} = 0.0065 \text{ GeV}^2. \quad (25)$$

This focusing effect is a beautiful manifestation of quantum mechanics. The intuitive interpretation is rather straightforward. The condition that the neutron in the deuteron remains intact while the proton must interact means that the neutron tries to pass the nucleus through the diluted periphery while the proton prefers the collision to be central. These conflicting conditions cause a strong suppression of small-size deuteron fluctuations, while large separations in the deu-

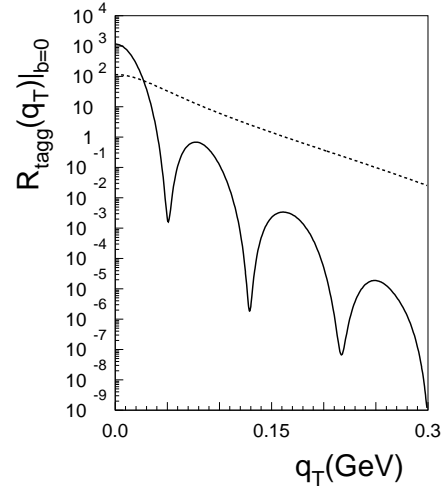


FIG. 6. Same as in Fig. 5, but for a central ($b=0$) proton-gold collision, accompanied by a spectator neutron.

teron are enhanced. Apparently, such large-size configurations are related to a smaller Fermi momentum and this simple observation explains the focusing effect.

This explanation offers a possibility to study the correlation of the focusing effect with centrality of collision.⁴ Suppressing b integration in Eq. (21) one can trace the b dependence of the focusing effect. In Fig. 6 the same comparison of two q_T distributions is shown for central collision $b=0$ (impact parameter of the interacting proton). The interpretation of central collisions is especially clear. Once the proton hits the center of the nucleus, the spectator neutron must be located along a ring outside the nucleus with a radius larger than the nucleus. Correspondingly, the q_T distribution has the typical diffractive shape and a small width $\Delta q_T \approx 1/R_A$.

Contrary to our expectations, the distributions are quite similar. The mean value of $\langle q_T^2 \rangle = 0.00032 \text{ GeV}^2$ is close to our result, Eq. (24), for the minimal bias sample.

One may wonder why the minima on the q_T distribution, Fig. 6, are deeper than for the minimal bias sample, Fig. 5. In fact, for central collisions the minima go down to zero, since we neglect the real part of the elastic amplitude and the Fourier transform oscillates changing sign. However, the position of the minima (slightly) depends on the impact parameter of the collision. Therefore, when one sums up q_T distributions with different minimum positions, the resulting distribution will have minima which are partially filled up.

One should be cautious when comparing these predictions with data which might be contaminated by nonspectator neutrons. First, the neutron calorimeters used at RHIC have a rather large acceptance which covers transverse momenta up to $\sim 300 \text{ MeV}$. Therefore, most of the neutrons which experienced quasielastic scattering contribute as well (except STAR). Besides, the range of longitudinal momenta is rather large and events with diffractive excitation on nucleons in the gold should contribute, too. All such neutrons are not spectators and have much wider q_T distribution.

⁴I am thankful to Alexei Denisov for this suggestion.

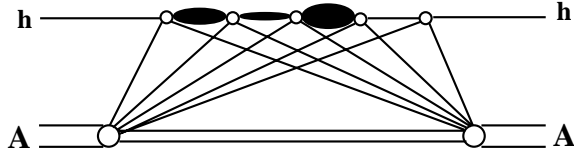


FIG. 7. Diagonal and off-diagonal diffractive multiple interactions of the projectile hadron in intermediate state.

Second, selecting central collisions in accordance with higher multiplicity, one should remember that central collisions are suppressed (see Fig. 3) and one should not mix them up with the fluctuations of multiplicity.

IV. INELASTIC SHADOWING CORRECTIONS

A. Intermediate state diffractive excitations

The Glauber model is a single-channel approximation, it misses the possibility of diffractive excitation of the projectile in the intermediate state illustrated in Fig. 7. These corrections, called inelastic shadowing, were introduced by Gribov back in 1969 [9]. The formula for the inelastic corrections to the total hadron-nucleus cross section was suggested in Ref. [18],

$$\begin{aligned} \Delta\sigma_{tot}^{hA} = & -4\pi \int d^2b \exp\left[-\frac{1}{2}\sigma_{tot}^{hN}T_A(b)\right] \\ & \times \int_{M_{min}^2} dM^2 \frac{d\sigma_{sd}^{hN}}{dM^2 dp_T^2} \Big|_{p_T=0} \int_{-\infty}^{\infty} dz_1 \rho_A(b, z_1) \\ & \times \int_{z_1}^{\infty} dz_2 \rho_A(b, z_1) e^{iq_L(z_2-z_1)}, \end{aligned} \quad (26)$$

where σ_{sd}^{hN} is the cross section of single diffractive dissociation $hN \rightarrow XN$ with longitudinal momentum transfer

$$q_L = \frac{M^2 - m_h^2}{2E_h}. \quad (27)$$

This correction makes nuclei more transparent [19]. One can also see from Fig. 1 that Eq. (26) does a good job describing data at low energies [10,20], since it takes care of the onset of inelastic shadowing via phase shifts controlled by q_L . Higher order off-diagonal transitions are neglected. Diagonal transitions (or absorption of the excited state) are important, but unknown. Indeed, the intermediate state X has definite mass M , but no definite size, or cross section. It is *ad hoc* fixed in Eq. (26) at σ_{tot}^{hN} . It has been a long standing problem of how to deal simultaneously with phase shifts which are controlled by the mass and with the cross section which depends on the size. This problem was eventually solved in Refs. [21,22] within the light-cone Green function approach (see Sec. VI).

The situation changes at the high energies of RHIC and LHC, all multiple interactions become important, but phase shifts vanish, substantially simplifying calculations. No experimental information, however, is available for off-

diagonal diffractive amplitudes for excited state transitions $X_1 \rightarrow X_2$. A solution proposed in Ref. [23] is presented in the following section.

There is, however, one exclusion which is free from these problems, hadron-deuteron collisions. In this case no interaction in the intermediate state is possible and knowledge of diffractive cross section $NN \rightarrow NX$ is sufficient to calculate the inelastic correction with no further assumptions. In this case Eq. (26) takes the simple form [9,24], analogous to Eq. (A17),

$$\Delta\sigma_{tot}^{hd} = -2 \int dM^2 \int dp_T^2 \frac{d\sigma_{sd}^{hN}}{dM^2 dp_T^2} F_d(t). \quad (28)$$

We calculate this correction for pd collisions following Ref. [25] at $\sqrt{s}=200$ GeV using the slope $B_{NN}^{sd}=10$ GeV⁻² which is reduced by the proton vertex contribution 4 GeV⁻² compared to $B_{NN}^{el}=14$ GeV⁻². The upper cutoff imposed by the deuteron form factor on integration over M^2 is quite high at this energy and we can use the free-diffraction cross section $\sigma_{sd}^{NN}=4$ mb [12]. Then we find $\Delta\sigma_{tot}^{hd}=-1.75$ mb.

B. Eigenstate method

If a hadron were an eigenstate of interaction, i.e., could undergo only elastic scattering (as a shadow of inelastic channels) and no diffractive excitation was possible, the Glauber formula would be exact and no inelastic shadowing corrections would be needed. This simple observation gives a hint that one should switch from the basis of physical hadronic states to a new one consisting of a complete set of mutually orthogonal states, which are eigenstates of the scattering amplitude operator. This was the driving idea of description of diffraction in terms of elastic amplitudes [26,27], and becomes a powerful tool for calculation of inelastic shadowing corrections in all orders of multiple interactions [23]. Hadronic states (including leptons and photons) can be decomposed into a complete set of such eigenstates $|k\rangle$,

$$|h\rangle = \sum_k \Psi_k^h |k\rangle, \quad (29)$$

where Ψ_k^h are hadronic wave functions in the form of Fock state decomposition. They obey the orthogonality conditions

$$\sum_k (\Psi_k^{h'})^\dagger \Psi_k^h = \delta_{hh'},$$

$$\sum_h (\Psi_h^h)^\dagger \Psi_k^h = \delta_{hk}. \quad (30)$$

We denote by $f_{el}^{kN} = i \sigma_{tot}^{kN}/2$ the eigenvalues of the elastic amplitude operator \hat{f} neglecting its real part. We assume that the amplitude is integrated over impact parameter, i.e., the forward elastic amplitude is normalized as $|f_{el}^{kN}|^2 = 4\pi d\sigma_{el}^{kN}/dt|_{t=0}$. We can then express the elastic $f_{el}(hh)$ and off-diagonal diffractive $f_{sd}(hh')$ amplitudes as

$$f_{el}^{hN} = 2i \sum_k |\Psi_k^h|^2 \sigma_{tot}^{kN} \equiv 2i\langle\sigma\rangle; \quad (31)$$

$$f_{sd}^{hN}(h \rightarrow h') = 2i \sum_k (\Psi_k^{h'})^\dagger \Psi_k^h \sigma_{tot}^{kN} \quad (32)$$

Note that if all the eigenamplitudes were equal, the diffractive amplitude (32) would vanish due to the orthogonality relation, Eq. (30). The physical reason is obvious. If all the f_{el}^{kN} are equal, the interaction does not affect the coherence between the different eigencomponents $|k\rangle$ of the projectile hadron $|h\rangle$. Therefore, off-diagonal transitions are possible only due to differences between the eigenamplitudes.

If one sums up all final states in the diffractive cross section, one can use the completeness condition (30). Then, excluding the elastic channels one gets [23,28,29]

$$16\pi \left. \frac{d\sigma_{sd}^{hN}}{dt} \right|_{t=0} = \sum_i |\Psi_i^h|^2 \langle \sigma_{tot}^{iN} \rangle^2 - \left(\sum_i |\Psi_i^h|^2 \sigma_{tot}^{iN} \right)^2 \equiv \langle \sigma_{tot}^2 \rangle - \langle \sigma_{tot} \rangle^2. \quad (33)$$

As long as the main problem of the Glauber approximation is the need to include off-diagonal transitions, one should switch to an eigenstate basis. Then each of the eigenstates can experience only elastic diffractive scatterings and the Glauber eikonal approximation becomes exact. Thus, all the expressions for cross sections of different channels derived in the Glauber approximation in Appendix A are exact for any of the eigenstates. Then, the corresponding cross sections for hadron-nucleus collisions are obtained via a proper averaging of those in Appendix A [23,29],

$$\sigma_{tot}^{hA} = 2 \int d^2b \{ 1 - \langle \exp[-\frac{1}{2} \sigma_{tot} T_A^h(b)] \rangle \}, \quad (34)$$

$$\sigma_{el}^{hA} = \int d^2b | 1 - \langle \exp[-\frac{1}{2} \sigma_{tot} T_A^h(b)] \rangle |^2, \quad (35)$$

$$\sigma_{in}^{hA} = \int d^2b \{ 1 - \langle \exp[-\sigma_{in} T_A^h(b)] \rangle \}. \quad (36)$$

It is interesting that the last expression for σ_{in}^{hA} is already free from diffraction contribution. Although only elastic and quasielastic cross sections were subtracted from σ_{tot}^{hA} in Glauber model in Appendix A, after averaging over eigenstates it turns out that diffraction is subtracted as well. Indeed, direct averaging of the elastic cross section, Eq. (A9), is different from Eq. (35) and includes coherent diffraction, $hA \rightarrow XA$, in which cross section reads [23,29]

$$\sigma_{sd}^{hA}(hA \rightarrow XA) = \int d^2b \{ \langle \exp[-\sigma_{tot} T_A^h(b)] \rangle - \langle \exp[-\frac{1}{2} \sigma_{tot} T_A^h(b)] \rangle^2 \}. \quad (37)$$

Averaging of the quasielastic cross section, Eq. (A13), leads to inclusion of diffractive excitation of the hadron $h \rightarrow X$ besides excitation of the nucleus, $A \rightarrow Y$.

Thus, Eq. (36), resulting from a direct averaging of the single-channel inelastic cross section Eq. (A14), corresponds to that part of the total hA cross section which does not contain elastic scattering, $hA \rightarrow hA$, coherent diffraction, hA

$\rightarrow XA$, quasielastic, $hA \rightarrow hY$, and double diffraction, $hA \rightarrow XY$. This part of the cross section is what is measured as the inelastic cross section in heavy ion and $p(d)A$ collisions at SPS and RHIC, and what we are going to calculate below.

One may wonder, what is the difference between the cross sections in Eqs. (34) and (36) and those in Glauber approximation, Eqs. (A5), (A9), and (A14)? The difference is obvious, in the former set of equations the exponentials are averaged, while the Glauber approximation contains exponentials of averaged values. For instance, the total cross section in the Glauber approximation reads

$$\sigma_{tot}^{hA}|_{GI} = 2 \int d^2b \{ 1 - \exp[-\frac{1}{2} \langle \sigma_{tot}^i \rangle T_A^h(b)] \}, \quad (38)$$

where $\langle \sigma_{tot} \rangle = \sigma_{tot}^{hN}$. If we subtract this from Eq. (34), the rest is Gribov's inelastic correction calculated in all orders. Indeed, we can compare it with expression (34) expanding the exponentials in Eqs. (34) and (38) in multiplicity of interactions up to the lowest order. Employing Eq. (33) we find

$$\begin{aligned} \sigma_{tot}^{hA} - \sigma_{tot}^{hA}|_{GI} &= \int d^2b \frac{1}{4} [\langle \sigma_{tot}^i \rangle^2 - \langle (\sigma_{tot}^i)^2 \rangle] T_A^h(b)^2 \\ &= -4\pi \int d^2b T_A^h(b)^2 \int dM^2 \left. \frac{d\sigma_{sd}^h}{dM^2 dt} \right|_{t=0}. \end{aligned} \quad (39)$$

This result is identical to Eq. (26), if we neglect there the phase shift vanishing at high energies and also expand the exponential.

Note that since the inelastic nuclear cross section in the form of Eq. (A14) is correct for eigenstates, one may think that averaging this expression would give the correct answer. However, such a procedure includes a possibility of excitation of the projectile and disintegration of the nucleus to nucleons, but misses the possibility of diffractive excitation of bound nucleons which is not a small correction. We introduce a corresponding correction in the following section.

V. LIGHT-CONE DIPOLES AND INELASTIC SHADOWING

A. Excitation of the valence quark skeleton

The light-cone dipole representation in QCD was introduced in Ref. [29] where it was realized that color dipoles are the eigenstates of interaction and can be an effective tool for calculation of diffraction and nuclear shadowing. It was concluded that the key quantity of the approach, the cross section of the dipole-nucleon, $\sigma_{qq}^N(r_T)$, is a universal and flavor independent function which depends only on transverse separation r_T and energy. Of course the energy must be sufficiently high to freeze variations of the dipole size during interaction, otherwise one should rely on the Green function approach [30,21,22] (see Sec. VI).

This representation suggests an effective way to sum up all multistep inelastic corrections in all orders [29]. Since dipoles are eigenstates of interaction in QCD, they are not

subject to any diffractive excitation, and the eikonal approximation becomes exact. Therefore, if energy is high enough to keep the transverse size of a dipole “frozen” by Lorentz time dilation during propagation through the nucleus, one can write the cross sections in the form of Eqs. (34)–(36). The averaging in this case means summing up different Fock components of the hadron consisting of different numbers of quarks and gluons, and for each of them integration is over r_T (intrinsic separations), weighted with the square of the hadron light-cone wave function $|\Psi_h(r_T)|^2$. We assume that the hadron does not have a “molecular” structure, i.e., is not like a deuteron consisting of two colorless clusters. Therefore all the following expressions apply only to elementary hadrons. To simplify calculations, in what follows, we rely on the quark-diquark model of the proton, neglecting the diquark size. The total cross section is basically insensitive to the diquark size, besides, there are many evidences that this size is indeed small [31,32].

1. Nuclear transparency

According to the Glauber model hadrons attenuate exponentially in nuclear matter,

$$\text{Tr} = \exp(-\sigma_{tot}^{hN} T_A), \quad (40)$$

where Tr, called nuclear transparency, is the survival probability of a hadron propagating through a nuclear matter of thickness T_A . However, we know that the hadron fluctuates and can be viewed as a combination of Fock states of different content and size. Some of them having a small transverse size can easily penetrate the medium and do not attenuate as fast as in Eq. (40).

Assuming that the hadronic wave function has a Gaussian form and the dipole cross section $\sigma(r_T) \propto r_T^2$ (this small- r_T behavior does a good job describing hierarchy of hadronic cross sections and their sizes [33]) we can perform averaging in Eq. (34) and arrive at a rather simple expression [29]

$$\langle \exp[-\sigma(r)T_A] \rangle = \frac{1}{1 + \sigma_{tot}^{hN} T_A}. \quad (41)$$

This explicitly demonstrates how Gribov’s corrections make nuclei more transparent. Since exponential attenuation is much stronger than a power, for large T_A (central collisions with heavy nuclei) the difference might be tremendous.

2. Cross sections

The total cross section. The total hadron-nucleus cross section is modified according to Eq. (41) as

$$\sigma_{tot}^{hA} = \int d^2b \frac{\sigma_{tot}^{hN} T_A^h(b)}{1 + \frac{1}{2} \sigma_{tot}^{hN} T_A^h(b)}. \quad (42)$$

Although Gribov’s corrections (color transparency) make nuclei much more transparent, the modified total cross section, Eq. (42), is not much smaller than the result of the Glauber approximation, Eq. (A5). This is because the central area of a heavy nucleus is “black,” i.e., fully absorptive, in both cases, and the cross section is mainly related to the

geometry of the nucleus. In other words, the exponential term in Eq. (A5) is very small for central collisions, and the total cross section is rather insensitive to even dramatic variations of its magnitude.

The elastic cross section. The partial elastic cross section is given by the square of the averaged value of the elastic amplitude. We get

$$\sigma_{el}^{hA} = \frac{1}{4} \int d^2b \frac{[\sigma_{tot}^{hN} T_A^h(b)]^2}{[1 + \frac{1}{2} \sigma_{tot}^{hN} T_A^h(b)]^2}. \quad (43)$$

Correspondingly, the differential elastic cross section reads

$$\frac{d\sigma_{el}^{hA}}{dq_T^2} = \frac{1}{16\pi} \left| \int d^2b \frac{\sigma_{tot}^{hN} T_A^h(b)}{1 + \frac{1}{2} \sigma_{tot}^{hN} T_A^h(b)} \exp(i\vec{q} \cdot \vec{b}) \right|^2. \quad (44)$$

The total inelastic cross section. The cross section of all inelastic channels is given by the difference

$$\sigma_{in}^{hA} = \sigma_{tot}^{hA} - \sigma_{el}^{hA} = \int d^2b \frac{\sigma_{tot}^{hN} T_A^h(b) [1 + \frac{1}{4} \sigma_{tot}^{hN} T_A^h(b)]}{[1 + \frac{1}{2} \sigma_{tot}^{hN} T_A^h(b)]^2}. \quad (45)$$

This cross section approaches the unitarity limit for $\sigma_{tot}^{hN} T_A^h(b) \gg 1$ at the nuclear center, but is proportional to $T_A^h(b)$ at the nuclear periphery.

Diffractive excitation of the hadron. The combined cross section of elastic scattering and diffraction when the hadron may be either excited or not, but the nucleus remains intact, is given by the average of the dA elastic partial amplitude squared:

$$\sigma_{sd+el}^{hA}(hA \rightarrow XA) = \frac{1}{2} \int d^2b \frac{[\sigma_{tot}^{hN} T_A^h(b)]^2}{[1 + \sigma_{tot}^{hN} T_A^h(b)][1 + \frac{1}{2} \sigma_{tot}^{hN} T_A^h(b)]}. \quad (46)$$

Here we first averaged over the quark coordinates in the nucleons, second, squared the result, and third, subtracted the elastic dA cross section [compare with Eq. (37)].

Diffractive excitation of the nucleus. The cross section of the reaction where the nucleus is diffractively excited, and the hadron either remains intact or is excited, too, reads

$$\sigma_{qel}^{hA}(hA \rightarrow XA^*) = \int d^2b \frac{2\tilde{\sigma}_{el}^{hN} T_A^h(b)}{[1 + \sigma_{tot}^{hN} T_A^h(b)]^3}, \quad (47)$$

where

$$\begin{aligned} \tilde{\sigma}_{el}^{hN} = & \sigma_{el}^{hN} + \sigma_{sd}^{hN}(hN \rightarrow XN) + \sigma_{sd}^{hN}(hN \rightarrow hY) \\ & + \sigma_{dd}^{hN}(hN \rightarrow XY), \end{aligned} \quad (48)$$

and σ_{sd}^{hN} is a cross section of single diffractive excitation of either the beam or the target; the double diffractive cross section σ_{dd}^{hN} corresponds to diffractive excitation of both.

Deriving Eq. (47) we made use of the smallness of the elastic cross section and expanded the exponential. Higher orders of σ_{el}^{hN} are neglected, but the corrections are easy to

calculate. We also neglected the small variation of the elastic slope of the dipole-nucleon cross section with r_T .

Equation (47), as one can see from Eq. (48), takes into account the possibility of diffractive excitation of the projectile. This is a direct consequence of the eigenstate approach. In addition, we also included the possibility of diffractive excitation of bound nucleons in the target. These excitations are not shadowed by multiple interactions in the nucleus, since all extra particles produced in this way stay in the nuclear fragmentation region and do not break down the large rapidity gap structure of the event. Therefore, they may be incorporated into $\tilde{\sigma}_{el}^{hN}$ adding the last two terms. At $\sqrt{s} = 200$ GeV single and double diffraction cross sections are about equal, $\sigma_{sd}^{NN} \approx \sigma_{dd}^{NN} \approx 4$ mb [12,13], $\sigma_{el}^{NN} \approx 9$ mb, so $\tilde{\sigma}_{el}^{NN} \approx 21$ mb.

Diffractive reactions, Eqs. (47) and (48), do not produce any particles at central rapidities. Therefore, if one wants to calculate the part of the total hadron-nucleus cross section detected experimentally, one should subtract these diffractive contributions,

$$\begin{aligned} \tilde{\sigma}_{in}^{hA} &= \sigma_{tot}^{hA} - \sigma_{sd+el}^{hA}(hA \rightarrow XA) - \sigma_{qel}^{hA}(hA \rightarrow XA^*) \\ &= \int d^2b \frac{\sigma_{tot}^{hN} T_A^h(b)}{1 + \sigma_{tot}^{hN} T_A^h(b)} \left\{ 1 - \frac{2\tilde{\sigma}_{el}^{hN} / \sigma_{tot}^{hN}}{[1 + \sigma_{tot}^{hN} T_A^h(b)]^2} \right\}. \end{aligned} \quad (49)$$

Since pp cross section is used as a baseline for comparison, the same subtraction should be done in this case, too,

$$\tilde{\sigma}_{in}^{pp} = \sigma_{tot}^{NN} - \tilde{\sigma}_{el}^{NN}, \quad (50)$$

which comes to about $\tilde{\sigma}_{in}^{pp} = 30$ mb at $\sqrt{s} = 200$ GeV.

Then, the number of collisions at a given impact parameter corrected for inelastic shadowing reads

$$N_{coll}(b) = \frac{\tilde{\sigma}_{in}^{NN}}{\sigma_{tot}^{NN}} [1 + \sigma_{tot}^{NN} T_A^h(b)] \left\{ 1 - \frac{\tilde{\sigma}_{el}^{NN} / \sigma_{tot}^{NN}}{[1 + \sigma_{tot}^{NN} T_A^h(b)]^2} \right\}^{-1}. \quad (51)$$

B. Deuteron-nucleus collisions

So far we considered the case of colorless hadrons, but colored constituents. The specifics of a deuteron is that it contains two colorless clusters, nucleons. Therefore, one of the inelastic corrections which we already took into account in Eq. (7) is related to fluctuations of the deuteron size. The next step is to average over the fluctuations of the sizes of the nucleons.

The total deuteron-nucleus cross section. Now we should average σ_{tot}^{dA} over the internucleon separation, as well as over the nucleon sizes \vec{r}_1 and \vec{r}_2 ,

$$\sigma_{tot}^{dA} = 2 \int d^2b \int d^2r_T |\Psi_d(r_T)|^2 \langle f^{dA}(\vec{b}, \vec{r}_T) \rangle_{r_1, r_2}, \quad (52)$$

where

$$\langle f^{dA}(\vec{b}, \vec{r}_T) \rangle_{r_1, r_2} = 1 - \frac{1}{[1 + \frac{1}{2} \sigma_{tot}^{NN} T_A^N(\vec{b} + \frac{1}{2} \vec{r}_T)][1 + \frac{1}{2} \sigma_{tot}^{NN} T_A^N(\vec{b} - \frac{1}{2} \vec{r}_T)]} - \frac{\sigma_{el}^{NN} T_A^N(b) \exp\left(-\frac{r_T^2}{4B_{NN}}\right)}{[1 + \frac{1}{2} \sigma_{tot}^{NN} T_A^N(\vec{b} + \frac{1}{2} \vec{r}_T)]^2 [1 + \frac{1}{2} \sigma_{tot}^{NN} T_A^N(\vec{b} - \frac{1}{2} \vec{r}_T)]^2}. \quad (53)$$

The result of calculation exposed in Table I is smaller than the Glauber model value. The difference comes from inelastic shadowing related to diffractive excitations of the colorless clusters in the deuteron, each consisting of three valence quarks.

Elastic and diffractive scattering of deuterons. Correspondingly, the total cross section of elastic scattering and diffractive excitation of the deuteron has the form

$$\sigma_{el}^{dA} + \sigma_{sd}^{dA}(dA \rightarrow XA) = \int d^2b \int d^2r_T |\Psi_d(r_T)|^2 \langle g^{dA}(\vec{b}, \vec{r}_T) \rangle_{r_1, r_2}, \quad (54)$$

where

$$\begin{aligned} \langle g^{dA}(\vec{b}, \vec{r}_T) \rangle_{r_1, r_2} &= 1 - \frac{2}{[1 + \frac{1}{2} \sigma_{tot}^{NN} T_A^N(\vec{b} + \frac{1}{2} \vec{r}_T)][1 + \frac{1}{2} \sigma_{tot}^{NN} T_A^N(\vec{b} - \frac{1}{2} \vec{r}_T)]} + \frac{2\sigma_{el}^{NN} T_A^N(b) \exp\left(-\frac{r_T^2}{4B_{NN}}\right)}{[1 + \sigma_{tot}^{NN} T_A^N(\vec{b} + \vec{r}_T)]^2 [1 + \sigma_{tot}^{NN} T_A^N(\vec{b} - \frac{1}{2} \vec{r}_T)]^2} \\ &+ \frac{1}{[1 + \sigma_{tot}^{NN} T_A^N(\vec{b} + \vec{r}_T)][1 + \frac{1}{2} \sigma_{tot}^{NN} T_A^N(\vec{b} - \frac{1}{2} \vec{r}_T)]} - \frac{\sigma_{el}^{NN} T_A^N(b) \exp\left(-\frac{r_T^2}{4B_{NN}}\right)}{[1 + \sigma_{tot}^{NN} T_A^N(\vec{b} + \frac{1}{2} \vec{r}_T)]^2 [1 + \sigma_{tot}^{NN} T_A^N(\vec{b} - \frac{1}{2} \vec{r}_T)]^2}. \end{aligned} \quad (55)$$

Inelastic deuteron-nucleus collisions. If we subtract the elastic and diffractive cross section, Eq. (54), from Eq. (52) the rest will be the inelastic cross section which covers all diffractive excitations of the nucleus, but not gold. This is what is measured in the STAR experiment. To comply with the condition of experiments insensitive to diffraction one should also subtract the cross section of diffractive excitation of the nucleus. The results read [compare with Eq. (49)]

$$\tilde{\sigma}_{in}^{dA} = \sigma_{tot}^{dA} - \sigma_{el}^{dA} - \sigma_{sd}^{dA}(dA \rightarrow XA) - \sigma_{sd}^{dA}(dA \rightarrow dY) - \sigma_{dd}^{dA}(dA \rightarrow XY) = \int d^2b \int d^2r_T |\Psi_d(r_T)|^2 \langle h^{dA}(\vec{b}, \vec{r}_T) \rangle_{r_1, r_2}, \quad (56)$$

where

$$\langle h^{dA}(\vec{b}, \vec{r}_T) \rangle_{r_1, r_2} = \left\{ 1 - \frac{1}{[1 + \sigma_{tot}^{NN} T_A^N(\vec{b} + \frac{1}{2}\vec{r}_T)][1 + \sigma_{tot}^{NN} T_A^N(\vec{b} - \frac{1}{2}\vec{r}_T)]} - \frac{2\tilde{\sigma}_{el}^{NN} T_A^N(\vec{b} + \frac{1}{2}\vec{r}_T)}{[1 + \sigma_{tot}^{NN} T_A^N(\vec{b} + \frac{1}{2}\vec{r}_T)]^3 [1 + \sigma_{tot}^{NN} T_A^N(\vec{b} - \frac{1}{2}\vec{r}_T)]} \right. \\ \left. - \frac{2\tilde{\sigma}_{el}^{NN} T_A^N(\vec{b} - \frac{1}{2}\vec{r}_T)}{[1 + \sigma_{tot}^{NN} T_A^N(\vec{b} + \frac{1}{2}\vec{r}_T)][1 + \sigma_{tot}^{NN} T_A^N(\vec{b} - \frac{1}{2}\vec{r}_T)]^3} - \frac{2\sigma_{el}^{NN} T_A^N(b) \exp(-\frac{r_T^2}{4B_{NN}})}{[1 + \sigma_{tot}^{NN} T_A^N(\vec{b} + \frac{1}{2}\vec{r}_T)]^2 [1 + \sigma_{tot}^{NN} T_A^N(\vec{b} - \frac{1}{2}\vec{r}_T)]^2} \right\}. \quad (57)$$

The results of calculations of both inelastic cross sections with and without nuclear diffraction, as well as the corresponding numbers of collisions which are rather small compared to what was calculated in Ref. [1], are presented in Table I. As expected, the cross sections are smaller than predicted by the Glauber model, while the numbers of collisions are larger. We also plotted b dependence of σ_{in}^{dA} in Fig. 2 (thin solid curve). Comparing with the Glauber curve we see that this class of the inelastic shadowing corrections leave the mid of nucleus black, but make it rather transparent on the periphery.

Production of spectator nucleons. Similarly, one derives an equation for the cross section of a channel with tagged spectator nucleons corrected for inelastic shadowing,

$$\sigma_{tagg}^{d-Au} = \int d^2b \int d^2r_T \frac{|\Psi_d(r_T)|^2}{1 + \sigma_{tot}^{NN} T_A^N(\vec{b} + \frac{1}{2}\vec{r}_T)} \\ \times \left\{ 1 - \frac{1}{1 + \sigma_{tot}^{NN} T_A^N(\vec{b} - \frac{1}{2}\vec{r}_T)} \right. \\ \left. - \frac{2\tilde{\sigma}_{el}^{NN} T_A^N(\vec{b} - \frac{1}{2}\vec{r}_T) + 2\sigma_{el}^{NN} T_A^N(b) \exp[-r_T^2/4B_{NN}]}{[1 + \sigma_{tot}^{NN} T_A^N(\vec{b} + \frac{1}{2}\vec{r}_T)]^3} \right\}. \quad (58)$$

Events with tagged nucleons are especially sensitive to the transparency of the nucleus. We calculated the cross section, Eq. (58), and the results of these as well as those of corresponding numbers of collisions are shown in Table I. The effect of inelastic corrections on the impact parameter distribution of interacting protons in tagged events with a spectator neutron is demonstrated in Fig. 3. Calculation was done for inelastic proton interaction including diffractive excitations (STAR). As one could anticipate, the nucleus becomes much more transparent in the center. Indeed, for a nearly black nucleus inelastic corrections keep it black since transparency or the exponential term is so small that even if it is modified by a large factor, the final change is very small. However, tagged event is a direct measure of transparency,

and the inelastic corrections are maximal in this case. It is not surprising that N_{coll} is quite large (considering that only one nucleon interacts).

C. Towards realistic calculations

1. Three valence quarks

For the sake of simplicity we used so far the approximation of a quark-diquark structure of the proton and neglected the diquark size. Indeed, as long as the diquark is as small as 0.2–0.3 fm [31,32], this approximation is rather precise even for heavy nuclei which can hardly resolve such a small size. However, the mean size of the isoscalar diquark is still a debatable issue; besides, an isovector diquark is probably a big object. Then, one may expect nuclear matter to be more opaque for a high-energy nucleon compared to what was found above.

We evaluate nuclear transparency for another extreme, i.e., for the case of a proton wave function symmetric in all quark coordinates, with a mean size of any diquark of the order of 0.7 fm:

$$|\Psi_N(\vec{r}_1, \vec{r}_2, \vec{r}_3)|^2 = \frac{3}{(\pi r_N^2)^2} \exp\left(-\frac{r_1^2 + r_2^2 + r_3^2}{r_N^2}\right) \delta(\vec{r}_1 + \vec{r}_2 + \vec{r}_3). \quad (59)$$

To perform the averaging of the eikonal exponentials in Eqs. (34)–(36) we need to know the three-body dipole cross section, which we express via the conventional $\bar{q}q$ one as

$$\sigma_{3q}(\vec{r}_1, \vec{r}_2, \vec{r}_3) = \frac{1}{2}[\sigma_{\bar{q}q}(r_1) + \sigma_{\bar{q}q}(r_2) + \sigma_{\bar{q}q}(r_3)]. \quad (60)$$

It satisfies the limiting conditions, that is, it turns into $\sigma_{\bar{q}q}(r)$ if one of the three separations is zero. Assuming that $\sigma_{\bar{q}q}(r) = Cr^2$, this cross section averaged with the wave function squared, Eq. (59), gives $\sigma_{tot}^{NN} = Cr_N^2/2$.

Now we can calculate the nuclear transparency averaging the eikonal exponential

$$\begin{aligned}
 \langle \exp[-\sigma_{3q}(r_i)T_A(b)] \rangle &= \int \prod_i^3 d^2r_i |\Psi_N(\vec{r}_1, \vec{r}_2, \vec{r}_3)|^2 \\
 &\quad \times \exp[-\sigma_{3q}(\vec{r}_1, \vec{r}_2, \vec{r}_3)T_A(b)] \\
 &= \frac{1}{[1 + \frac{1}{2}\sigma_{tot}^{NN}T_A(b)]^2} \quad (61)
 \end{aligned}$$

We see that nuclear transparency in this case is a quadratic, rather than a linear function of the inverse nuclear thickness. For small $\sigma_{tot}^{NN}T_A(b) \ll 1$ it coincides with the result of the quark-diquark model, Eq. (41), however it falls steeper at large $T_A(b)$. This is not surprising; in order to make use of color transparency the whole proton has to fluctuate into a small transverse area, and it is more probable for a two-body system than for a three-body system.

One can consider these results as a lower [Eq. (61)] and an upper [Eq. (41)] bound for nuclear transparency. We calculated different cross sections using the average of the eikonal exponential in the form of Eq. (61) instead of Eq. (41), and the results are shown in Table I in parenthesis. Unfortunately, we still do not know the proton wave function sufficiently well to fix this uncertainty for nuclear transparency. Nevertheless, the difference is not large for real nuclei. For instance, the inelastic nondiffractive d -Au cross section presented in Table I increases by about 6%.

2. Realistic dipole cross section

The dipole cross section $\sigma_{qq}^N \propto r_T^2$ used above is justified only for small r_T , while it is expected to level off at large $\bar{q}q$ separations. More reliable calculations can be done using a realistic phenomenological cross section. A quite popular parametrization was proposed in Ref. [34] and fitted to HERA data for $F_2(x, Q^2)$. However, it should not be used for our purpose, since it is unable to provide the correct energy dependence of hadronic cross sections; namely, the pion-proton cross section cannot exceed 23 mb.⁵

A parametrization more appropriate for soft hadronic physics was proposed in Ref. [11]:

$$\sigma_{qq}(r_T, s) = \sigma_0(s) \left[1 - \exp\left(-\frac{r_T^2}{R_0^2(s)}\right) \right], \quad (62)$$

where $R_0(s) = 0.88 \text{ fm } (s_0/s)^{0.14}$ and $s_0 = 1000 \text{ GeV}^2$. In contrast to Ref. [34] all values depend on energy (as it is supposed to be for soft interactions) rather than on x , and the energy dependent parameter $\sigma_0(s)$ is defined as

$$\sigma_0(s) = \sigma_{tot}^{\pi p}(s) \left(1 + \frac{3r_0^2(s)}{8\langle r_{ch}^2 \rangle_\pi} \right). \quad (63)$$

Here $\langle r_{ch}^2 \rangle_\pi = 0.44 \pm 0.01 \text{ fm}^2$ [35] is the mean square of the pion charge radius. Cross section (62) averaged with the

⁵According to Ref [35] this dipole cross section reproduced well the energy dependence of the photoabsorption cross section $\sigma_{tot}^{\gamma p}(s)$. This happens only due to the singularity in the light-cone wave function of the photon at small r_T . This is a specific property of the transverse photon wave function and is not applicable to hadrons.

pion wave function squared automatically reproduces the pion-proton cross section. The pp total cross section is also well reproduced using the quark-diquark approximation for the proton wave function. The parameters are adjusted to HERA data for the proton structure function. Agreement is quite good up to at least $Q^2 \sim 10 \text{ GeV}^2$ sufficient for our purposes.

With such a dipole cross section one can perform analytic calculations expanding the Glauber exponentials in Eq. (34) and (37). Then the total cross section gets the form

$$\sigma_{tot}^{hA} = 2 \int d^2b \left\{ 1 - \exp\left[-\frac{1}{2}\sigma_0(s)T_A^h(b)\right] \sum_{n=0}^{\infty} \frac{[\sigma_0(s)T_A^h(b)]^n}{2^n n! (1+n\delta)} \right\}. \quad (64)$$

Correspondingly, the sum of elastic and diffractive deuteron scattering on the nucleus reads

$$\begin{aligned}
 \sigma_{sd+el}^{hA}(hA \rightarrow XA) &= \int d^2b \left\{ 1 + \exp\left[-\frac{1}{2}\sigma_0(s)T_A^h(b)\right] \right. \\
 &\quad \times \sum_{n=0}^{\infty} \frac{[\sigma_0(s)T_A^h(b)]^n}{n! (1+n\delta)} \\
 &\quad \left. \times \left(1 - 2^{1-n} \exp\left[-\frac{1}{2}\sigma_0(s)T_A^h(b)\right] \right) \right\}. \quad (65)
 \end{aligned}$$

The cross section of quasielastic excitation of the nucleus with simultaneous possibility to excite the deuteron is given by

$$\begin{aligned}
 \sigma_{qe}^{hA}(hA \rightarrow XA^*) &= \int d^2b \exp\left[-\frac{1}{2}\sigma_0(s)T_A^h(b)\right] \\
 &\quad \times \sum_{n=0}^{\infty} \frac{[\sigma_0(s)T_A^h(b)]^n}{n!} \\
 &\quad \times \frac{2\delta^2}{[1+n\delta][1+(n+1)\delta][1+(n+2)\delta]}. \quad (66)
 \end{aligned}$$

In all these equations

$$\delta = \frac{8\langle r_p^2 \rangle}{3R_0^2(s)}. \quad (67)$$

Now one can calculate $\tilde{\sigma}_{in}^{hA}$ subtracting Eqs. (65) and (66) from Eq. (64). However, in this paper we restrict ourselves by calculations performed above and leave this more complicated computation for further study.

VI. GLUON SHADOWING AND THE TRIPLE-POMERON DIFFRACTION

First of all, to avoid confusion it should be emphasized that we are not talking about gluon shadowing in high- p_T hadron production at $x_F=0$ in d -Au collisions. This process exploits Bjorken $x > 0.01$ which is too large for gluon shad-

owing [4,11]. On the contrary, we consider gluon shadowing in the soft inelastic d -Au collisions which is the main contributor to the total cross section. This process is related to much smaller $x \sim 10^{-5}$.

Gluon shadowing is an important source of inelastic corrections at very high energies. It is pretty clear if one employs Eq. (26). The part of the diffraction which corresponds to the triple-Regge graph PPR, or the lowest order Fock component consisting only of valence quarks, has a steep M dependence, $d\sigma_{sd}^{hN}/dM^2 \propto 1/M^3$. Therefore the integral over M^2 in Eq. (26) well converges, the minimal momentum transfer q_L vanishes at high energies, and this part of inelastic corrections saturates.

The triple-Pomeron (PPP) part of diffraction which corresponds to the Fock state containing at least one gluon is divergent at large masses, $d\sigma_{sd}^{hN}/dM^2 \propto 1/M^2$, since the gluon is a vector particle. The cut off is imposed by the nuclear form factor in Eq. (26), i.e., the condition $q_L \lesssim 1/R_A$. As a result of the divergence, this part of the inelastic corrections rises as $\ln(s/s_0)$ and reaches a substantial value at the energy of RHIC.

Eikonalization of the lowest Fock state $|3q\rangle$ of the proton done in Eqs. (34)–(36) corresponds to the Bethe-Heitler regime of gluon radiation. Indeed, gluon bremsstrahlung is responsible for the rising energy dependence of the phenomenological cross section (62), and in the eikonal form (34)–(36) one assumes that the whole spectrum of gluons is multiply radiated. However, the Landau-Pomeranchuk-Migdal (LPM) effect [37,38] is known to suppress radiation in multiple interactions. Since the main part of the inelastic cross section at high energies is related to gluon radiation, the LPM effect becomes a suppression of the cross section. This is a quantum-mechanical interference phenomenon and is a part of the suppression called Gribov's inelastic shadowing. The way it is taken into account in the QCD dipole picture is inclusion of higher Fock states, $|3qG\rangle$, etc. Each of these dipoles is of course colorless and its elastic amplitude on a nucleon is subject to eikonalization.

As already mentioned, Eq. (26) should not be used at high energies as it misses all higher order multiple off-diagonal transitions, and incorrectly (*ad hoc*) calculates diagonal ones. On the other hand, the eigenstate expressions, Eqs. (34)–(36), are not safe to use either. Indeed, the significant part of the integral over M^2 in Eq. (26), next to the upper cutoff, corresponds to a finite q_L . In other words, the fluctuation *valence quarks + gluons* is not frozen by Lorentz time dilation during propagation through the nucleus.

A. The Green function for glue-gluon dipoles

A proper treatment of a quark-gluon fluctuation “breathing” during propagation through a nucleus is offered by the light-cone Green function formalism. In this approach the absorption cross section as well as the phase shifts are functions of longitudinal coordinate. This is also a parameter-free description, all the unknowns are fixed by comparison with other data. We employ this approach and calculate gluon shadowing following Ref. [11].

The key point which affects further calculations is the nonperturbative light-cone wave function of the quark-gluon Fock state,

$$\Psi_{qG}(\vec{r}) = \frac{2}{\pi} \sqrt{\frac{\alpha_s}{3}} \frac{\vec{e} \cdot \vec{r}}{r^2} \exp\left(-\frac{r^2}{2r_0^2}\right). \quad (68)$$

Here we assume (as usual) that the gluon is carrying a negligible fraction, $\alpha_G \ll 1$, of the quark momentum. This wave function is quite different from the perturbative one which is the same as in light-cone description of the Drell-Yan process [39,11]. The latter, employed for calculation of diffractive gluon radiation (the triple-Pomeron term), results in overestimation of data for large mass diffraction by more than an order of magnitude. This problem has been known since 1970s as the puzzle of smallness of the triple-Pomeron coupling. The way out is to make a natural assumption that the parent light-front quark and gluon experience a nonperturbative interaction which squeezes that quark-gluon wave packet and therefore reduces the dipole cross section. The parameter r_0 in Eq. (68) controls the strength of the real part of the light-cone potential which is chosen in a Gaussian form. Fit to diffractive data $pp \rightarrow pX$ leads to the value of the mean transverse q - G separation $\sqrt{\langle r^2 \rangle} \equiv r_0 = 0.3$ fm. This conclusion goes along with the results of nonperturbative models, such as the instanton vacuum model [40] and lattice calculations [41], which found a similar small size for gluonic fluctuations. Such a semihard scale $1/r_0$ also leads to quite a steep energy behavior of the radiation cross section and well explains data for the total and differential elastic cross sections of pp scattering [42].

Apparently, smallness of r_0 leads to quite a weak shadowing for Fock states containing gluons. As a consequence, we expect rather weak gluon shadowing, which is not a surprise in view of the close connection between diffraction and shadowing. As long as the gluon clouds around valence quarks are small, Gribov's corrections are suppressed. Besides, the fluctuations containing gluons become heavy and the onset of gluon saturation takes place at much smaller x than usually expected.

The mean quark-gluon separation $r_0 \approx 0.3$ fm is much smaller than the quark separation in light hadrons. For this reason one can neglect the interferences between the amplitudes of gluon radiation by different valence quarks. Since the gluon contribution to the cross section corresponds to the difference between the amplitudes of $|qqqG\rangle$ and $|qqq\rangle$ components, the spectator quarks cancel out. Then the radiation cross section is controlled by the quark-gluon wave function and the color octet (GG) dipole cross section.

Thus, the contribution to the total hadron-nucleus cross section which comes from gluon radiation has the form

$$\sigma_G^{hA} = \int_x^1 \frac{d\alpha_G}{\alpha_G} \int d^2b P(\alpha_G, \vec{b}), \quad (69)$$

where α_G is the fraction of the quark momentum carried by the gluon,

$$\begin{aligned}
 P(\alpha_G, \vec{b}) = & T_A(b) \int d^2r |\Psi_{qG}(\vec{r}, \alpha_G)|^2 \sigma_{GG}(r, s) \\
 & - \frac{1}{2} \text{Re} \int_{-\infty}^{\infty} dz_1 dz_2 \Theta(z_2 - z_1) \rho_A(b, z_1) \rho_A(b, z_2) \\
 & \times \int d^2r_1 d^2r_2 \Psi_{qG}^*(\vec{r}_2, \alpha_G) \sigma_{GG}(r_2, s) \\
 & \times G_{GG}(\vec{r}_2, z_2; \vec{r}_1, z_1) \sigma_{GG}(r_1, s) \Psi_{qG}(\vec{r}_1, \alpha_G).
 \end{aligned} \tag{70}$$

Here the energy and Bjorken x are related as $s=2m_N E_q = 4/xr_0^2$.

The second term in Eq. (70) corresponds to the triple-Pomeron part of the inelastic correction, Eq. (26), written in impact parameter representation. The amplitude of diffractive gluon radiation $qN \rightarrow GqN$ is proportional to $\Psi_{qG}(\vec{r}, \alpha_G) \sigma_{GG}(r)$. A glue-gluon dipole emerges in this expression because this is not elastic scattering but a production process. Its amplitude comes from the difference of the scattering amplitudes of different Fock components of the quark [39], $|q\rangle$ and $|qG\rangle$, which is a dipole cross section of a color octet-octet dipole, $\bar{q}q-G$. Since the size of the $\bar{q}q$ pair is irrelevant for gluon shadowing, we neglect it and replace the $\bar{q}q$ by a gluon (see in Refs. [43,11]). Therefore the second term in Eq. (70) can be interpreted as production of a qG pair at the point z_1 and then as propagation of this pair with varying transverse separation up to point z_2 where it converts back to the quark.

Propagation of the dipoles of varying sizes through the absorptive medium between points z_1 and z_2 is described by the Green function $G_{GG}(\vec{r}_2, z_2; \vec{r}_1, z_1)$. It satisfies the two-dimensional Schrödinger equation

$$\begin{aligned}
 i \frac{d}{dz_2} G_{GG}(\vec{r}_2, z_2; \vec{r}_1, z_1) = & \left[- \frac{\Delta(\vec{r}_2)}{2E_q \alpha_G (1 - \alpha_G)} \right. \\
 & \left. + V(\vec{r}_2, z_2) \right] G_{GG}(\vec{r}_2, z_2; \vec{r}_1, z_1),
 \end{aligned} \tag{71}$$

where imaginary part of the light-cone potential is related to absorption in the medium,

$$\text{Im} V(\vec{r}, z) = -\frac{1}{2} \sigma_{GG}(\vec{r}) \rho_A(b, z). \tag{72}$$

For further calculations we assume that the quark energy is $E_q = s/6m_N$, but the results are hardly sensitive to this approximation.

Perturbative calculations treating a quark-gluon fluctuation as free particles overestimates the cross section of diffractive gluon radiation (or the triple-Pomeron coupling) by more than an order of magnitude. The only way to suppress this cross section is to reduce the mean transverse size of the fluctuation. This is done in Ref. [11] via introduction of a real part of the light-cone potential in Eq. (71),

$$\text{Re } V(\vec{r}, z) = \frac{r^2}{2E_q r_0^4 \alpha_G (1 - \alpha_G)}, \tag{73}$$

where parameter r_0 was fitted to data for single diffraction $pp \rightarrow pX$.

The gluonic dipole cross section $\sigma_{GG}(r, s)$ is assumed to be different from the $\bar{q}q$ one, Eq. (62), only by the Casimir factor 9/4. To simplify calculations we rely on the small- r approximation, $\sigma_{GG}(r, s) \approx C_{GG}(s) r^2$, where $C_{GG}(s) = d \sigma_{GG}(r, s) / d r^2_{r=0}$. This approximation for the dipole cross section is justified by the small value of $r_0^2 \approx 0.1 \text{ fm}^2$.

In the case of a constant nuclear density, $\rho_A(r) = \rho_A \Theta(R_A - r)$, the solution of Eq. (71) has the form

$$\begin{aligned}
 G_{GG}(\vec{r}_2, z_2; \vec{r}_1, z_1) = & \frac{A}{2\pi \sinh(\Omega \Delta z)} \\
 & \times \exp \left\{ -\frac{A}{2} \left[(r_1^2 + r_2^2) \coth(\Omega \Delta z) \right. \right. \\
 & \left. \left. - \frac{2\vec{r}_1 \cdot \vec{r}_2}{\sinh(\Omega \Delta z)} \right] \right\},
 \end{aligned} \tag{74}$$

where

$$A = \frac{1}{r_0^2} \sqrt{1 - i \alpha_G (1 - \alpha_G) E_q C_{GG} \rho_A r_0^4}$$

$$\Omega = \frac{iA}{\alpha_G (1 - \alpha_G) E_q},$$

$$\Delta z = z_2 - z_1. \tag{75}$$

Integrations in Eq. (70) can be performed analytically,

$$P(\alpha_G, \vec{b}) = \frac{4\alpha_G}{3\pi} \text{Re} \ln(W), \tag{76}$$

where

$$W = \cosh(\Omega L) + \frac{A^2 r_0^2 + 1}{2A} \sinh(\Omega L), \tag{77}$$

$$L = 2\sqrt{R_A^2 - b^2}. \tag{78}$$

The first term in Eq. (70) is a part of the nuclear cross section calculated in the Bethe-Heitler limit, i.e., without gluonic inelastic shadowing. Therefore it is included in the nuclear cross sections calculated so far. The new inelastic shadowing correction comes from the second term in Eq. (70). Its fraction of the total pA cross section is depicted in Fig. 8. The onset of shadowing is delayed up to $\sqrt{s} \sim 20 \text{ GeV}$. We believe that this result is trustable since the Green function approach treats phase shifts and attenuation in nuclear matter consistently. Nevertheless, in order to get an idea about the scale of theoretical uncertainty we also evaluated the magnitude of gluon shadowing using the known values of the triple-Pomeron coupling and Eq. (26). The results are quite similar, in both cases the gluon shadowing correction is pretty small [11], $\sim 20\%$ at the energy of

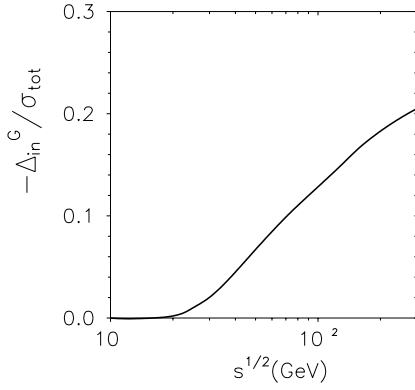


FIG. 8. Ratio of the gluonic inelastic shadowing correction (minimal bias) to the total nuclear cross section as function of center of mass energy \sqrt{s} .

RHIC. Such a weak shadowing is a direct result of smallness of the parameter $r_0=0.3$ fm which we use. This seems to be the only way to suppress diffractive gluon radiation corresponding to the triple-Pomeron contribution and to reach agreement with data on diffractive dissociation $pp \rightarrow pX$. For this reason, all effects related to gluons, including saturation, or color-glass condensate, are quite suppressed.

Naturally, the inelastic correction in Eqs. (70) and (77) varies with impact parameter vanishing on the very periphery and reaching a maximum at central collisions. At small $T_A(b)$ the inelastic correction is proportional to $T_A^2(b)$ while the partial amplitude is proportional to $T_A(b)$. Therefore, the ratio linearly rises with $T_A(b)$ (see in Refs. [44,45]) with a coefficient approximately equal to 0.2 fm^2 . For very large $T_A^2(b)$ the correction may even exceed the rest of the cross section, then apparently higher order corrections must be added to stop this growth. Such a saturation is not important for real nuclei, therefore we use the linear parametrization $R_G(b)=1-\Delta_{in}^G(b)=1-0.2 T_A(b)$ for further calculations.

The valence quark part of the inelastic shadowing corrections makes the nucleus more transparent, i.e., it reduces the elastic scattering amplitude as one can explicitly see comparing the corrected amplitude, Eq. (42), with the Glauber form, Eq. (A5). However, both approach the black disk limit for large $T_A(b)\sigma_{tot}^{NN} \gg 1$. An important question is whether this is still true after inclusion of gluonic corrections.

Equation (70) has the typical form of a nonlinear equation such as Glibov-Levin-Ryskin (GLR) evolutions equation [45], or in the dipole form Balitsky-Kovchegov (BK) equation [46]. The second term on the right-hand side of Eq. (70) corresponds to glue-gluon fusion in GLR equation or the multiple interaction in the nucleus in BK equations. We calculated the correction in the lowest order using the uncorrected dipole cross section $\sigma_{GG}(r)$, i.e., the undisturbed free gluon density. Next iterations would be to implement the corrected gluon density (at larger x , however), or $\sigma_{GG}(r)$, into the second term in Eq. (70). This procedure leads to the BK equation whose solution is still a challenge. However, due to smallness of the correction, 20%, we do not expect large higher order corrections and the saturated solution should not be very different from our result which we employ in further applications.

On the other hand, if gluon shadowing emerging from the first order iteration is very strong, as it was found in Refs. [48–50], it should be substantially reduced by next iterations which effectively play the role of self-screening; namely, as long as the gluon density is reduced at small x , one cannot use in Eq. (26) the cross section of diffractive dissociation on a free nucleon target. It is suppressed by the same gluon shadowing, (at larger x though). The stronger is the gluon shadowing the more important is this self-screening effect. It was missed in calculations [48–50] which grossly overpredicted the strength of gluon shadowing.

Now we are in a position to correct our previous calculations for the gluonic part of inelastic shadowing which we fix at 20%. We do it replacing $\sigma_{qq}(r_T) \Rightarrow R_G(b)\sigma_{qq}(r_T)$, where $R_G(b)=1-\Delta_{in}(b)$ is the suppression factor related to gluon shadowing. This simple prescription is based on the intuitive expectation that a dipole interacts with a lesser number of gluons in the nucleus than the eikonal model assumes. Indeed, for small separations r_T , the dipole cross section reads [51] $\sigma_{qq}(r_T)=(\pi^2/3)\alpha_s r_T^2 G(x, r_T)$, i.e., it is indeed proportional to the gluon density which is reduced in nuclei. More motivations for this procedure can be found in Refs. [44,45].

The results for nuclear cross sections corrected for gluon shadowing are shown in Table I and depicted in Figs. 2–4 by thick solid curves.

B. More models for gluon shadowing

Although we predict quite a modest gluon shadowing effect and therefore a rather small inelastic shadowing correction, many models predict much stronger effects. One can call it theoretical uncertainty if one treats all models equally (though some of them are probably more equal than others [52]).

For instance, the popular event generator HIJING contains a Q^2 -independent gluon shadowing [53] which is a factor of 0.3 at $x \sim 10^{-5}$. With such a dramatic gluon shadowing we get the impact parameter dependence of the inelastic cross section depicted by dotted curve in Fig. 2. The corresponding correction factor $K=0.65$ for the PHENIX data.

If we treat shadowing in terms of the dipole approach, it is clear that shadowing is a monotonic function of Q^2 , since the size of the dipole can only rise towards the soft limit. This is confirmed by Dokshitzer-Gribov-Lipatov-Altarelli-Parisi (DGLAP) evolution of nuclear shadowing in the perturbative domain. Therefore, one can use gluon shadowing predicted by different models at the starting scale Q_0 of the order of $1-2 \text{ GeV}^2$ as a bottom bound for the shadowing correction expected in the soft limit. We calculate Bjorken x for the RHIC energy $\sqrt{s}=200 \text{ GeV}$ and $Q^2=1 \text{ GeV}^2$.

A strong gluon shadowing was predicted in Refs. [48,49], $R_G=0.3-0.4$. HERA data for diffraction $\gamma^* p \rightarrow Xp$ were used as an input in Eq. (26) modified for $\gamma^* A$ collisions. The statistics of these data are much lower than in proton diffraction $pp \rightarrow pX$ and not sufficient for reliable determination of the triple-Pomeron coupling. Different solutions for this coupling fitted to deep-inelastic scattering (DIS) diffractive data vary dramatically [54]. Besides, as is mentioned above, the gluon self-screening missed in Refs. [48,49] should significantly reduce the effect of gluon shadowing.

Explicit calculations of gluon shadowing via gluon dipoles were performed in Ref. [50]. The gluon shadowing corresponding to the RHIC energies was found at $R_G \approx 0.6$ which leads to correction factor $K=0.78$ for the PHENIX ratio R_{dA} . This calculation also, however, does not include the gluon self-screening and is based on the assumption that gluon and quark dipoles have identical distribution functions.

A strong gluon suppression was also found in a model with an early onset of strong saturation [55] whose characteristic scale is a steep function of energy, $Q_s^2 \propto (1/x)^{0.252}$. It was assumed in the Kharzeev-Levin-McLerran approach [6] that for $Q^2 \leq Q_s^2$ gluon density $xG_A(x, Q^2)$ is proportional to $Q^2 R_A^2$ with a factor which was taken from the McLerran-Venugopalan model [56] at $x=10^{-1}$. Such an oversimplified picture exhibits a strong gluon shadowing. If we compare the $xG_A(x, Q^2)$ with the Gluck-Reya-Vogt (GRV) parametrization [57] at $x \sim 10^{-4}$ it turns out to be strongly suppressed by factor $R_G=0.42$. In this case the correction factor in Eq. (5) is $K=0.72$.

Such a diversity of model predictions suggests a conclusion that the current data for deuteron-gold collisions [1–3] cannot resolve in a model independent way the dilemma whether final state interaction or initial conditions is the main source of hadron suppression in heavy ion collisions. Indeed, if the latter were true, it would unavoidably lead to a substantial reduction of σ_{in}^{NA} and the ratio, Eq. (5) (compared to the Glauber model).

C. Number of participants

Although the concept of number of participants originates from a naive treatment of multiparticle production called wounded nucleon model, it is a widely used characteristic of centrality of collisions. We are not going to dispute here its meaning, but just to see how it is affected by the inelastic corrections⁶ relying on its formal definition,

$$\left. \frac{dN_p(s, b)}{d^2b} \right|_{Gl} = T_A(\vec{s} - \vec{b}) \{1 - \exp[-\sigma_{in}^{NN} T_B(b)]\} + T_B(s) [1 - \exp\{-\sigma_{in}^{NN} T_A(\vec{s} - \vec{b})\}], \quad (79)$$

where \vec{s} is the parameter of collision of nuclei A, B . We use subscript Gl to emphasize that it corresponds to this model which is inspired by the Glauber model (although they have nothing in common).

Apparently, inelastic shadowing corrections should reduce N_p since nuclear matter becomes more transparent. The corrected expression for N_p reads

$$\frac{dN_p(s, b)}{d^2b} = \sigma_{in}^{NN} T_A(\vec{s} - \vec{b}) T_B(b) \times \left\{ \frac{R_G(b)}{1 + R_G(b) \sigma_{in}^{NN} T_B(b)} + \frac{R_G(\vec{s} - \vec{b})}{1 + R_G(\vec{s} - \vec{b}) \sigma_{in}^{NN} T_A(\vec{s} - \vec{b})} \right\}. \quad (80)$$

Here the gluon shadowing factor R_G is a function of im-

⁶I am thankful to Larry McLerran, who suggested to look at this parameter

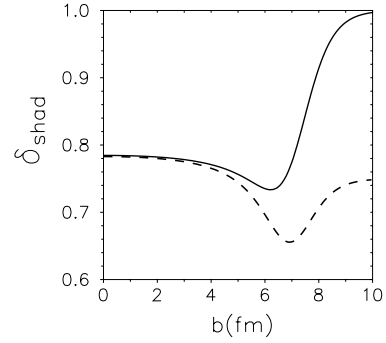


FIG. 9. Solid line is the correction factor, Eq. (81), for inelastic shadowing to the number of participants in p -Au collisions as a function of impact parameter. Dashed curve also includes a correction to σ_{in}^{NN} (see text).

pact parameter according to calculations in Refs. [11,44,45] and the parametrization used above. We present the correction to the ‘‘Glauber’’ expression defined as

$$\delta_{shad}(b) = \frac{R_G(b) \sigma_{in}^{NN} T_B(b)}{1 + R_G(b) \sigma_{in}^{NN} T_B(b)} \Big/ \{1 - \exp[-\sigma_{in}^{NN} T_B(b)]\} \quad (81)$$

in Fig. 9 depicted by solid curve. As one could expect, the correction factor peaks at the nuclear periphery and approaches one at large impact parameters.

If we compare with Glauber calculations employing the incorrect inelastic cross section $\sigma_{in}^{NN}=42$ mb, the correction is even larger, as is demonstrated by dashed curve in Fig. 9.

VII. CRONIN EFFECT: RENORMALIZING THE DATA

Cronin effect for high- p_T pions at $\sqrt{s}=200$ GeV was predicted in Ref. [4] to be a rather small enhancement, about 10% at the maximum. The smallness of the effect is due to the change of the mechanism of high- p_T particle production which takes place at the RHIC energies. At lower energies (SPS, CERN) different bound nucleons contribute to this hard process incoherently. The nuclear enhancement is due to initial/final state p_T broadening of partons propagating through the nucleus. This broadening should not be translated into a modification of the parton distribution in the nucleus since k_T factorization is broken [58]. At high energy an incoming light-cone fluctuation which contains a high- p_T parton is freed via coherent interaction with many nucleons in the target. It turns out that such a coherent mechanism leads to a weaker Cronin enhancement than the incoherent one. This is why calculations [59,60] missing this effect of coherence predict a stronger Cronin effect.

The PHENIX data for neutral pions [1] are depicted in Fig. 10 by full points in comparison with the predicted ratio [4]. However, as it was stressed above, the normalization of the data is based on Glauber model calculations which are subject to different corrections, all of which have negative sign. As a result, the data should be renormalized according

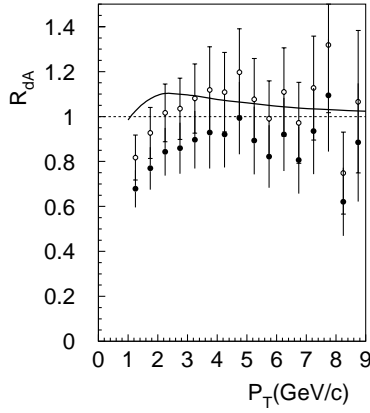


FIG. 10. The Cronin ratio $R_{Au/d}(p_T)$ for pions. Open circles show the results of PHENIX with normalization base upon Glauber model calculations of the inelastic d -Au cross section using $\sigma_{in}^{NN} = 42$ mb [1]. Full points show the same data corrected for a proper value of inelastic NN cross section and Gribov's inelastic shadowing. The error bars include statistic and systematic uncertainties. The curve is the prediction from Ref. [4].

to Table I by multiplying the experimental values by coefficient $K=0.83$. The corrected data are shown by open circles.

Cronin effect on a deuteron. Theoretical predictions have been done so far for pA collisions. In order to compare models with dA data one should make sure that the Cronin enhancement on the deuteron itself is a small correction. We evaluate the ratio

$$R_{pd}(p_T) = \frac{d\sigma^{pd}/d^2p_T}{2d\sigma^{pp}/d^2p_T}, \quad (82)$$

in the limit of short coherence length which gives an upper estimate for the effect. Following Ref. [4] the pd cross section at high p_T is given by the following convolution:

$$\sigma_{pd}(p_T) = \sum_{i,j,k,l} \tilde{F}_{i/p} \otimes F_{j/d} \otimes \hat{\sigma}_{ij \rightarrow kl} \otimes D_{h/k}, \quad (83)$$

where $F_{i/p}$ and $F_{j/d}$ are the distributions of parton species i, j dependent on Bjorken $x_{1,2}$ and transverse momenta of partons in the colliding proton and deuteron, respectively. The beam parton distribution \tilde{F}_i^p is modified by the transverse momentum broadening of the projectile parton due to interaction with another nucleon in the deuteron. The broadening of the mean transverse momentum squared reads [61,17]

$$\Delta \langle k_T^2 \rangle = 2 \left. \frac{d\sigma_{qq}(r_T)}{dr_T^2} \right|_{r_T=0} \langle T \rangle, \quad (84)$$

where $\langle T \rangle$ is the mean nuclear (deuteron) thickness covered by the projectile parton before or after the hard collision,

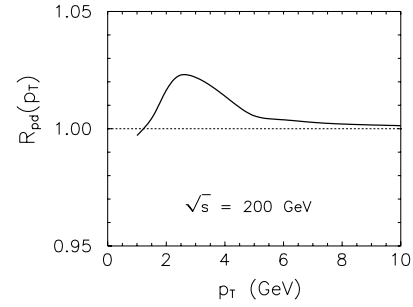


FIG. 11. Cronin ratio $R_{pd}(p_T)$ calculated at $\sqrt{s}=200$ GeV using the formalism developed in Ref. [4].

$$\langle T \rangle = \frac{2}{\sigma_{tot}^{hN}} \int d^2s \operatorname{Re} \Gamma^{hN}(s) |\Psi_d(s)|^2 \approx |\Psi_d(0)|^2, \quad (85)$$

where we neglected the elastic slope B_{NN} compared to the nuclear radius squared. For the parton distribution functions in a nucleon we use the leading order GRV parametrization [57].

We calculated this ratio using the computer code for the Cronin effect developed in Ref. [4],⁷ and the deuteron wave function $\Psi_d(\vec{r}_T)$ described in B.

The results for $R_{d/p}(p_T)$ are depicted in Fig. 11. Indeed, the Cronin enhancement is only 2%, and can be neglected comparing d -Au data with predictions done for p -Au.

VIII. SUMMARY AND CONCLUSIONS

The main observations and results of this paper are as follows.

(1) The current normalization of inclusive high- p_T cross section in deuteron-gold collisions measured at RHIC is based on Glauber model calculations of the inelastic d -Au cross section which is subject to Gribov's inelastic shadowing corrections. Importance of these corrections is not debatable, they have solid theoretical ground and are confirmed by precise measurements [1,20] (see Fig. 1). These corrections, Eq. (26), have negative sign, i.e., make nuclear medium more transparent, and they rise with energy.

(2) First of all, the Glauber calculations must be improved. The inelastic NN cross section used as an input should be corrected for diffraction. For experiments insensitive to diffraction (PHENIX, PHOBOS), the cross section should be reduced from $\sigma_{in}^{NN}=42$ mb down to $\tilde{\sigma}_{in}^{NN} \approx 30$ mb. On the contrary, if an experimental trigger detects diffraction (STAR), this cross section should be increased up to $\sigma_{tot}^{NN} = 51$ mb. This modification results in a correction factor K_{GI} presented in Table I.

(3) There are two types of inelastic shadowing corrections. One corresponds to diffractive excitation of the valence quark skeleton, or nucleonic resonances, and is related to the PPR triple-Regge graph. We calculated this correction,

⁷I am thankful to Jan Nemchik who performed this calculation for pd collisions.

Eqs. (42), (61), and (64), using the light-cone dipole representation which effectively sums up all orders of multiple interactions.

(4) Another type of inelastic shadowing is related to diffractive gluon bremsstrahlung or to the soft limit of gluon shadowing in nuclei related to the PPP triple-Pomeron diffractive. We performed calculations in Sec. VI using the solution for the Green function, Eq. (74), describing propagation of a glue-gluon dipole through nuclear medium and found a rather weak gluon shadowing for gold, about 20%. At the same time, other models predict much stronger gluon shadowing ranging up to corrections of 70% (Sec. VI B).

(5) Altogether, we expect a reduction of inelastic d -Au cross section compared to what was used for normalization of high- p_T data at RHIC. We conclude that the published data should be corrected by factor K which is about 0.8 for PHENIX and about 0.9 for STAR (see Table I). The renormalized data for pions do not possess any more the Cronin enhancement. This correction factor might be even smaller, down to 0.65, if we use a stronger gluon shadowing predicted by other models.

(6) One should admit that current data for high- p_T hadron production in d -Au collisions at RHIC cannot exclude in a model independent way the possibility of initial state suppression suggested in Ref. [6], although that would contradict the author's personal viewpoints.

(7) Probably the only way to settle this uncertainty is a direct measurement of either the cross section of high- p_T pion production in d -Au collisions or the inelastic d -Au cross sections at RHIC.

(8) A very sensitive test of models for inelastic shadowing offer tagged events with a spectator nucleon. In the situation where direct measurement of d -Au inelastic cross section is difficult, this might be a way to restrict models and narrow the band of theoretical uncertainty. The relative fraction of these events 20% measured in Ref. [2] create apparent problems for models with strong gluon shadowing which predict a much larger fraction. Even with our weak shadowing this fraction ranges between 23% and 26%. However, one should make sure that the detected neutrons are really spectators, which is not the case currently (see discussion in Sec. III).

(9) We found a beautiful quantum-mechanical effect: the nucleus acts like a lens focusing spectators. In spite of the naive anticipation that nucleons which escaped interaction retain their primordial Fermi momentum distribution, there is a strong narrowing effect substantially reducing the transverse momenta of the spectators. Besides, the distribution acquires the typical diffractive maxima and minima (see Figs. 5 and 6).

ACKNOWLEDGMENTS

This paper was written during a visit to Columbia University and I am thankful to Miklos Gyulassy and Alberto Accardi for hospitality and many inspiring discussions. I have also been much benefited from discussions with Barbara Jacak, Peter Levai, Ziwei Lin, Sasha Milov, Denes Molnar, Sergei Voloshin, and other participants of the workshop, as well as with Peter Braun-Munzinger, Claudio Ciofi, Alexei

Denisov, Jörg Hüfner, Yuri Ivanov, Berndt Müller, Andreas Schäfer, Mike Tannenbaum, and Xin-Nian Wang. My special thanks go to Yuri Ivanov and Irina Potashnikova for their kind assistance with numerical calculations. This work was supported by the grant from the Gesellschaft für Schwerionenforschung Darmstadt (GSI), Grant No. GSI-OR-SCH, and Grant No. INTAS-97-OPEN-31696.

APPENDIX A: GLAUBER MODEL GLOSSARY

The hA elastic amplitude at impact parameter b has the eikonal form

$$\Gamma^{hA}(\vec{b}; \{\vec{s}_j, z_j\}) = 1 - \prod_{k=1}^A [1 - \Gamma^{hN}(\vec{b} - \vec{s}_k)], \quad (\text{A1})$$

where $\{\vec{s}_j, z_j\}$ denote the coordinates of the target nucleon N_j . $i\Gamma^{hN}$ is the elastic scattering amplitude on a nucleon normalized as

$$\begin{aligned} \sigma_{tot}^{hN} &= 2 \int d^2b \operatorname{Re} \Gamma^{hN}(b), \\ \sigma_{el}^{hN} &= \int d^2b |\Gamma^{hN}(b)|^2. \end{aligned} \quad (\text{A2})$$

1. Heavy nuclei

In the approximation of single-particle nuclear density one can calculate a matrix element between the nuclear ground states:

$$\begin{aligned} \langle 0 | \Gamma^{hA}(\vec{b}; \{\vec{s}_j, z_j\}) | 0 \rangle &= 1 - \left[1 - \frac{1}{A} \int d^2s \Gamma^{hN}(s) \right. \\ &\quad \left. \times \int_{-\infty}^{\infty} dz \rho_A(\vec{b} - \vec{s}, z) \right]^A, \end{aligned} \quad (\text{A3})$$

where

$$\rho_A(\vec{b}_1, z_1) = \int \prod_{i=2}^A d^3r_i |\Psi_A(\{\vec{r}_j\})|^2 \quad (\text{A4})$$

is the nuclear single particle density.

Total cross section. The result, Eq. (A3), is related via unitarity to the total hA cross section

$$\begin{aligned} \sigma_{tot}^{hA} &= 2 \operatorname{Re} \int d^2b \left\{ 1 - \left[1 - \frac{1}{A} \int d^2s \Gamma^{hN}(s) T_A(\vec{b} - \vec{s}) \right]^A \right\} \\ &\approx 2 \int d^2b \left\{ 1 - \exp \left[-\frac{1}{2} \sigma_{tot}^{hN} (1 - i\rho_{pp}) T_A^h(b) \right] \right\}, \end{aligned} \quad (\text{A5})$$

where ρ_{pp} is the ratio of the real to imaginary parts of the forward pp elastic amplitude

$$T_A^h(b) = \frac{2}{\sigma_{tot}^{hN}} \int d^2s \operatorname{Re} \Gamma^{hN}(s) T_A(\vec{b} - \vec{s}) \quad (\text{A6})$$

and

$$T_A(b) = \int_{-\infty}^{\infty} dz \rho_A(b, z) \quad (\text{A7})$$

is the nuclear thickness function. We use exponential form of $\Gamma^{hN}(s)$ throughout the paper,

$$\text{Re } \Gamma^{hN}(s) = \frac{\sigma_{tot}^{hN}}{4\pi B_{hN}} \exp\left(\frac{-s^2}{2B_{hN}}\right), \quad (\text{A8})$$

where B_{hN} is the slope of the differential hN elastic cross section. Note that the accuracy of the optical approximation in Eq. (A5) is quite high for gold, $\sim 10^{-3}$, so we use it throughout the paper. We also neglect the real part of the elastic amplitude in what follows, since it gives a vanishing correction $\sim \rho_{pp}^2/A^{2/3}$.

Elastic cross section. As long as the partial elastic amplitude is known, the elastic cross section reads

$$\sigma_{el}^{hA} = \int d^2b \left| 1 - \exp\left[-\frac{1}{2}\sigma_{tot}^{hN} T_A^h(b)\right] \right|^2. \quad (\text{A9})$$

Total inelastic cross section. Apparently it is given by the difference between the total and elastic cross sections,

$$\sigma_{in}^{hA} = \sigma_{tot}^{hA} - \sigma_{el}^{hA} = \int d^2b \{1 - \exp[-\sigma_{tot}^{hN} T_A^h(b)]\}. \quad (\text{A10})$$

This includes all inelastic channels when either the hadron or the nucleus (or both) are broken up.

Quasielastic cross section. As a result of the collision the nucleus can be excited to a state $|F\rangle$. Summing over final states of the nucleus and applying the condition of completeness, one gets the quasielastic cross section

$$\begin{aligned} \sigma_{qel}^{hA} &= \sum_F \int d^2b [\langle 0 | \Gamma^{hA}(b) | F \rangle^\dagger \langle F | \Gamma^{hA}(b) | 0 \rangle - |\langle 0 | \Gamma^{hA}(b) | 0 \rangle|^2] \\ &= \int d^2b [\langle 0 | |\Gamma^{hA}(b)|^2 | 0 \rangle - |\langle 0 | \Gamma^{hA}(b) | 0 \rangle|^2]. \end{aligned} \quad (\text{A11})$$

Here we extracted the cross section of elastic scattering when the nucleus remains intact.

Then in the first term of this expression we make use of the relation

$$\begin{aligned} \text{Re} \int d^2s \frac{T_A^h(\vec{b}-\vec{s})}{A} \{1 - 2\Gamma^{hN}(s) + [\Gamma^{hN}(s)]^2\} \\ \approx 1 - \frac{1}{A} T_A^h(b) (\sigma_{tot}^{hN} - \sigma_{el}^{hN}), \end{aligned} \quad (\text{A12})$$

and arrive at

$$\sigma_{qel}^{hA} = \int d^2b \{ \exp[-\sigma_{in}^{hN} T_A^h(b)] - \exp[-\sigma_{tot}^{hN} T_A^h(b)] \}. \quad (\text{A13})$$

Inelastic nondiffractive cross section. If one is interested in the fraction of the total inelastic cross section (A10) which covers only reactions with production of new particles, one should exclude the nucleus breakup to nucleons and nuclear

fragments; that is, the quasielastic cross section, Eq. (A13),

$$\sigma_{prod}^{hA} = \int d^2b \{1 - \exp[-\sigma_{in}^{hN} T_A^h(b)]\}. \quad (\text{A14})$$

This additional subtraction makes sense only for experiments which miss the nonproduction breakup of the nucleus. If, however, all inelastic events are detected, including diffractive (production and nonproduction channels) excitations of the nucleus (check with Ref. [2]) one should rely on Eq. (A10) for the inelastic nuclear cross section.

Diffractive cross section. One needs to know this cross section in order to subtract it also from the inelastic cross section, since diffractive events escape registration at $p(d)A$ collisions at SPS and RHIC. The Glauber approximation is valid only for a single-channel problem. One can extend it to include diffraction properly introducing phase shifts due to longitudinal momentum transfer. However, one needs to know the cross section of interaction of the produced diffractive excitation with nucleons. This goes beyond the reach of the Glauber model, and instead of further ad hoc development of the model we solve this problem within the eigenstate method in Sec. IV B.

2. Proton-deuteron collisions

Apparently, Eq. (A5) should not be applied to light nuclei, in particular, to a deuteron. Instead one should use

$$\sigma_{tot}^{pd} = 2\sigma_{tot}^{NN} + \Delta\sigma_{tot}^{pd}, \quad (\text{A15})$$

where

$$\Delta\sigma_{tot}^{pd} = -2 \int d^2b \int d^2r_T |\Psi_d(r_T)|^2 \Gamma^{hN}(\vec{b} + \vec{r}_T/2) \Gamma^{hN}(\vec{b} - \vec{r}_T/2). \quad (\text{A16})$$

One can switch via Fourier transform to momentum representation in each of these three factors and perform integration over \vec{r}_T and \vec{b} . The result has a form of a one-dimensional integral [16],

$$\Delta\sigma_{tot}^{pd} = -\frac{2}{\pi} \int d^2q_T F_d(4q_T^2) \frac{d\sigma_{el}^{NN}}{dq_T^2}, \quad (\text{A17})$$

where $F_d(q^2)$ is the charge form factor of the deuteron. We neglected the correction $\sim 10^{-3}$ due to the nonzero real part of the forward NN amplitude. Note that \vec{s} in Eq. (A17) is the deuteron diameter, rather than the radius. This is why the form factor argument is $4q_T^2$.

We use parametrization of the deuteron form factor from Ref. [25],

$$F_d(q_T^2) = 0.55e^{-\alpha q_T^2} + 0.45e^{-\beta q_T^2}, \quad (\text{A18})$$

and $\alpha = 19.66 \text{ GeV}^{-2}, \beta = 4.67 \text{ GeV}^{-2}$.

Using $\sigma_{tot}^{NN} = 51 \text{ mb}$ at $\sqrt{s} = 200 \text{ GeV}$ and the elastic slope $B_{NN} = 14 \text{ GeV}^{-2}$, we found the total pd cross section $\sigma_{tot}^{pd} = 97 \text{ mb}$ with Glauber correction $\Delta_{GI}^{pd} = -5 \text{ mb}$. Since at this point a correct proton-deuteron cross section is needed, we

have to go beyond the Glauber approximation and add the inelastic correction considered in Sec. IV. We show that it is equivalent to adding the differential cross section of single diffraction, $pN \rightarrow XN$, to the elastic one in Eq. (A17). This increases the value of the shadowing correction by 1.75 mb. Finally, we arrive at the cross sections

$$\sigma_{tot}^{pd} = 95.15 \text{ mb},$$

$$\sigma_{in}^{pd} = \sigma_{tot}^{pd} - \frac{(\sigma_{tot}^{pd})^2}{16\pi B_{pd}} = 84.9 \text{ mb}. \quad (\text{A19})$$

Interestingly, the inelastic cross section is not affected by the Glauber correction, it is slightly larger than the sum of two inelastic NN cross sections. The slope from the differential elastic pd cross section was measured and fitted in Ref. [62],

$$\frac{d\sigma_{el}^{pd}}{dt} = \frac{(\sigma_{tot}^{pd})^2}{16\pi} e^{B_{pd}t + C_{pd}t^2}, \quad (\text{A20})$$

where

$$B_{pd} = b_0 + b_1 \ln s_{pd}, \quad (\text{A21})$$

with parameters $b_0 = 32.8 \pm 0.6$ (GeV^2) and $b_1 = 1.01 \pm 0.09$ (GeV^2). Parameter $C_{pd} = 54.0 \pm 0.9$ (GeV^{-2}) was found to be energy independent. At the energy of RHIC $B_{pd} = 44.1 \text{ GeV}^{-2}$, and we use this value in Eq. (A19).

The inelastic cross section, Eq. (A19), contains inelastic diffractive channels such as quasielastic breakup of the deuteron, $pd \rightarrow ppn$, and excitation of the nucleons $pd \rightarrow Xd$, $pd \rightarrow pY$, and $pd \rightarrow XY$. For the experiments insensitive to diffraction (PHENIX, PHOBOS) these channels must be subtracted.

APPENDIX B: DEUTERON WAVE FUNCTION AT REST AND LORENTZ BOOSTED

To perform calculations for interaction of a high-energy deuteron, one should not use the three-dimensional deuteron wave function, but needs to know the light-cone deuteron wave function expressed in Lorentz invariant variables, the transverse n - p separation \vec{r}_T and the light-cone fraction $\alpha = p_n^+ / p_d^+$ of the deuteron momentum carried by a nucleon. One cannot get this wave function by a simple Lorentz boost from the rest frame of the deuteron, where the three-dimensional wave function is supposed to be known, to the infinite momentum frame. Deuteron is not a classical system, under a Lorentz boost it acquires new constituents which are quantum fluctuations. These constituents buildup higher Fock components. This makes the procedure of Lorentz boost extremely complicated. There is, however, a practical

recipe suggested in Ref. [63] and is widely accepted. To the best of my knowledge, it works rather well for nonrelativistic systems (nuclei [64], heavy quarkonia [65], etc.)

The idea is straightforward to express the deuteron wave function in momentum representation,

$$\psi_d(\vec{q}) = \frac{1}{(2\pi)^3} \int d^3r e^{i\vec{q}\cdot\vec{r}} \psi_d(\vec{r}), \quad (\text{B1})$$

via the light-cone variables in the rest frame of the deuteron. To do it one should connect the three-dimensional momentum squared with the effective mass of the $c\bar{c}$ pair, $q^2 = M^2/4 - m_N^2$, expressed in terms of light-cone variables

$$M^2(\alpha, q_T) = \frac{q_T^2 + m_N^2}{\alpha(1-\alpha)}. \quad (\text{B2})$$

In order to change integration variable q_L to the light-cone α one uses their relation, $q_L = (\alpha - 1/2)M(q_T, \alpha)$, and gets a Jacobian which can be attributed to the definition of the light-cone wave function

$$\psi(\vec{q}) \Rightarrow \sqrt{2} \frac{(q^2 + m_N^2)^{3/4}}{(q_T^2 + m_N^2)^{1/2}} \cdot \psi(\alpha, \vec{q}_T) \equiv \Psi(\alpha, \vec{q}_T). \quad (\text{B3})$$

Applying this procedure to the S - and D -wave radial wave functions one gets

$$\frac{u(\vec{r})}{r} \Rightarrow U(\vec{r}_T, \alpha),$$

$$\frac{w(\vec{r})}{r} \Rightarrow W(\vec{r}_T, \alpha). \quad (\text{B4})$$

This dependence on α is important for exclusive final states, for instance, deuteron dissociation to nucleons with definite longitudinal momenta. However, for most applications in this paper we need to know the r_T retribution integrated over α ,

$$|\Psi_d(r_T)|^2 = \int_0^1 d\alpha [U^2(r_T, \alpha) + W^2(r_T, \alpha)], \quad (\text{B5})$$

The result of this is identical to the simple integration over longitudinal variable in the rest frame of the nucleus,

$$|\Psi_d(r_T)|^2 = \int_{-\infty}^{\infty} dr_L \frac{u^2(r) + w^2(r)}{r^2}. \quad (\text{B6})$$

We use the contemporary deuteron wave functions which employ the Nijmegen-93 potential [66].⁸

⁸I am grateful to Miklos Gyulassy for suggesting this and providing relevant data.

- [1] K. Adcox *et al.*, PHENIX Collaboration, Phys. Rev. Lett. **91**, 072303 (2003).
- [2] J. Adams *et al.*, STAR Collaboration, Phys. Rev. Lett. **91**, 072304 (2003); J. Adams *et al.*, nucl-ex/0305015
- [3] B. B. Back *et al.*, PHOBOS Collaboration, Phys. Rev. Lett. **91**, 072302 (2003).
- [4] B. Z. Kopeliovich, J. Nemchik, A. Schaefer, and A. V. Tarasov, Phys. Rev. Lett. **88**, 232303 (2002).
- [5] I. Vitev and M. Gyulassy, Phys. Rev. Lett. **89**, 252301 (2002).
- [6] D. Kharzeev, E. Levin, and L. McLerran, Phys. Lett. B **561**, 93 (2003).
- [7] D. Antreasyan *et al.*, Phys. Rev. D **19**, 764 (1979).
- [8] A. V. Abramovsky, V. N. Gribov, and O. V. Kancheli, Yad. Fiz. **18**, 595 (1973) [Sov. J. Nucl. Phys. **18**, 308 (1974)].
- [9] V. N. Gribov, Yad. Fiz. **9**, 640 (1969) [Sov. J. Nucl. Phys. **9**, 369 (1969)].
- [10] P. V. R. Murthy *et al.*, Nucl. Phys. **B92**, 269 (1975).
- [11] B. Z. Kopeliovich, A. Schäfer, and A. V. Tarasov, Phys. Rev. D **62**, 054022 (2000).
- [12] K. Goulios and J. Montanha, Phys. Rev. D **59**, 114017 (1999).
- [13] T. Affolder *et al.*, CDF Collaboration, Phys. Rev. Lett. **87**, 141802 (1991).
- [14] Barbara V. Jacak (private communication).
- [15] Michael J. Tannenbaum (private communication).
- [16] R. J. Glauber, Phys. Rev. **100**, 42 (1955).
- [17] M. B. Johnson, B. Z. Kopeliovich, and A. V. Tarasov, Phys. Rev. C **63**, 035203 (2001).
- [18] V. Karmanov and L. A. Kondratyuk, Sov. Phys. JETP **18**, 266 (1973).
- [19] B. Z. Kopeliovich and J. Nemchik, Phys. Lett. B **368**, 187 (1996).
- [20] A. Gsponer *et al.*, Phys. Rev. Lett. **42**, 9 (1979).
- [21] B. Z. Kopeliovich, J. Raufeisen, and A. V. Tarasov, Phys. Lett. B **440**, 151 (1998); J. Raufeisen, A. V. Tarasov, and O. O. Voskresenskaya, Eur. Phys. J. A **5**, 173 (1999).
- [22] B. Z. Kopeliovich, J. Raufeisen, and A. V. Tarasov, Phys. Rev. C **62**, 035204 (2000).
- [23] B. Z. Kopeliovich and L. I. Lapidus, Zh. Eksp. Teor. Fiz. **28**, 664 (1978) [JETP Lett. **28**, 614 (1978)].
- [24] J. Pumplin and M. Ross, Phys. Rev. Lett. **21**, 1778 (1968).
- [25] V. V. Anisovich, P. E. Volkovitsky, and L. G. Dakhno, Phys. Lett. **42B**, 224 (1972).
- [26] E. Feinberg and I. Ya. Pomeranchuk, Nuovo Cimento, Suppl. **3**, 652 (1956).
- [27] M. L. Good and W. D. Walker, Phys. Rev. **120**, 1857 (1960).
- [28] H. I. Miettinen and J. Pumplin, Phys. Rev. D **18**, 1696 (1978).
- [29] A. B. Zamolodchikov, B. Z. Kopeliovich, and L. I. Lapidus, Sov. Phys. JETP **33**, 612 (1981).
- [30] B. Z. Kopeliovich and B. G. Zakharov, Phys. Rev. D **44**, 3466 (1991).
- [31] M. Anselmino, E. Predazzi, S. Ekelin, S. Fredriksson, and D. B. Lichtenberg, Rev. Mod. Phys. **65**, 1199 (1993).
- [32] B. Z. Kopeliovich and B. G. Zakharov, Phys. Lett. B **211**, 221 (1988); Sov. J. Nucl. Phys. **48**, 136 (1988); Fiz. Elem. Chastits At. Yadra, **22**, 140 (1991) [Sov. J. Part. Nucl. **22**, 67 (1991)].
- [33] B. Povh and J. Hüfner, Phys. Rev. Lett. **58**, 1612 (1987).
- [34] K. Golec-Biernat and M. Wüsthoff, Phys. Rev. D **59**, 014017 (1999).
- [35] A. M. Stasto, K. Golec-Biernat, and J. Kwiecinski, Phys. Rev. Lett. **86**, 596 (2001).
- [36] S. Amendolia *et al.*, Nucl. Phys. **B277**, 186 (1986).
- [37] L. D. Landau and I. Ya. Pomeranchuk, Zh. Eksp. Teor. Fiz. **24**, 505 (1953); Dokl. Akad. Nauk SSSR **92**, 735 (1953); E. L. Feinberg and I. Ya. Pomeranchuk, *ibid.* **93**, 439 (1953); I. Ya. Pomeranchuk, *ibid.* **96**, 265 (1954); **96**, 481 (1954); E. L. Feinberg and I. Ya. Pomeranchuk, Nuovo Cimento, Suppl. **4**, 652 (1956).
- [38] A. B. Migdal, Phys. Rev. **103**, 1811 (1956).
- [39] B. Z. Kopeliovich, in *Proceedings of the Workshop on Dynamical Properties of Hadrons in Nuclear Matter*, Hirschegg, 1995, edited by H. Feldmeyer and W. Nörenberg (GSI, Darmstadt, 1995), p. 102, hep-ph/9609385
- [40] T. Schäfer and E. V. Shuryak, Rev. Mod. Phys. **70**, 323 (1998).
- [41] M. D'Elia, A. Di Giacomo, and E. Meggiolaro, Phys. Lett. B **408**, 315 (1997).
- [42] B. Z. Kopeliovich, I. K. Potashnikova, B. Povh, and E. Predazzi, Phys. Rev. Lett. **85**, 507 (2000); Phys. Rev. D **63**, 054001 (2001).
- [43] B. Z. Kopeliovich, A. Schäfer, and A. V. Tarasov, Phys. Rev. C **59**, 1609 (1999).
- [44] B. Z. Kopeliovich, J. Nemchik, A. Schaefer, and A. V. Tarasov, Phys. Rev. C **65**, 035201 (2002).
- [45] B. Z. Kopeliovich, J. Raufeisen, A. V. Tarasov, and M. B. Johnson, Phys. Rev. C **67**, 014903 (2003).
- [46] L. V. Gribov, E. M. Levin, and M. G. Ryskin, Nucl. Phys. **B188**, 555 (1981); Phys. Rep. **100**, 1 (1983).
- [47] I. I. Balitsky, Nucl. Phys. **B463**, 99 (1996); Yu. V. Kovchegov, Phys. Rev. D **60**, 034008 (1999).
- [48] L. Frankfurt and M. Strikman, Eur. Phys. J. A **5**, 293 (1999).
- [49] L. Frankfurt, V. Guzey, M. McDermott, and M. Strikman, J. High Energy Phys. **0202**, 027 (2002).
- [50] Z. Huang, H. J. Lu, and I. Sarcevic, Nucl. Phys. **A637**, 79 (1998).
- [51] B. Blättel *et al.*, Phys. Rev. Lett. **70**, 896 (1993).
- [52] G. Orwell, *Animal Farm*, Signet Classic (New American Library, New York, 1996).
- [53] S. y Li and X.-N. Wang, Phys. Lett. B **575**, 85 (2002).
- [54] L. Alvero, J. C. Collins, and J. J. Whitmore, Phys. Rev. D **59**, 074022 (1999); hep-ph/9806340.
- [55] E. M. Levin (private communication).
- [56] L. McLerran and R. Venugopalan, Phys. Rev. D **49**, 2233 (1994); **49**, 3352 (1994); **50**, 2225 (1994).
- [57] M. Gluck, E. Reya, and A. Vogt, Z. Phys. C **67**, 433 (1995).
- [58] G. T. Bodwin, S. J. Brodsky, and G. P. Lepage, Phys. Rev. D **39**, 3287 (1989).
- [59] X.-N. Wang, Phys. Rev. C **61**, 064910 (2000).
- [60] I. Vitev, Phys. Lett. B **562**, 36 (2003).
- [61] J. Dolejši, J. Hüfner, and B. Z. Kopeliovich, Phys. Lett. B **312**, 235 (1993).
- [62] Yu. Akimov *et al.*, Phys. Rev. D **12**, 3399 (1975); **15**, 2040(E) (1977).

- [63] M. V. Terent'ev, *Sov. J. Nucl. Phys.* **24**, 106 (1976).
- [64] L. Frankfurt and M. Strikman, *Phys. Rep.* **76**, 217 (1981);
160, 235 (1988).
- [65] J. Hüfner, Yu. P. Ivanov, B. Z. Kopeliovich, and A. V. Tarasov,
Phys. Rev. D **62**, 094022 (2000); *Phys. Rev. C* **66**, 024903 (2002).
- [66] V. G. J. Stoks, R. A. M. Klomp, C. P. F. Terheggen, and J. J. de Swart, *Phys. Rev. C* **49**, 2950 (1994).